Pergamon

Int. J. Solids Structures Vol. 35, Nos 26–27, pp. 3539–3571, 1998

0020–7683/98 $19.00 + .00

PII: S0020–7683(97)00232–1

ON BEHAVIOR OF PERFECT ELASTOPLASTICITY UNDER RECTILINEAR PATHS

H.-K. HONG* and C.-S. LIU
Department of Civil Engineering, Taiwan University, Taipei, Taiwan

(*Received* 6 *March* 1997; *in revised form* 11 *July* 1997)

Abstract—A perfect elastoplastic model for the relation of generalized stresses and their conjugate generalized strain rates is investigated in the paper. The exact solutions are solved for the model subjected to rectilinear generalized strain paths,[1] and the concepts of response subspace and visualization are introduced such that the n-dimensional problem is reduced to a two-dimensional problem in the response subspace. The response path is found to be, geometrically speaking, a geodesic in the n-dimensional closed ball $\mathbb{B}^n$ of generalized stresses. The phase portrait of dissipation is studied and it is a remarkable fact that in the response subspace the coordinate x is exactly the dissipation power per unit generalized strain rate when $x \geqslant x_{on}$ [see eqn (63)]. The generalized stress–strain curves are classified by geometrical shapes into ten types, in contrast to the superficial impression of only one type of shape, an inclined straight line followed by a horizontal line. The existence of a limit strength vector and a limit power of dissipation is demonstrated by the long-term behavior based on the exact solutions, and the existence together with the response's stability is further verified by Lyapunov's direct method. The closeness to the limit strength point is also estimated and the exact formula accounted for prestress is derived. The dependence of the responses on the product space of initial values, input paths, property constants and closeness to the limit is thoroughly investigated with control parameters identified.

1. INTRODUCTION AND MODEL

The paper analyzes critically the behavior of a model of perfect elastoplasticity subjected to rectilinear generalized strain paths. The response behavior including the switch-on time, limit strength vector, stability, generalized stress–strain curves, utlimate strength, peak strength, residual strength, dissipation, limit dissipation power, effect of generalized strain rates, asymptotic behavior, etc., is investigated in depth and illustrated geometrically. Although both the model and the paths investigated in the present paper seem rather simple, this critical study is considered to be fundamental and necessary for correctly attributing phenomena observed in experiments to appropriate models, and conversely it may help avoid an incorrect interpretation whatsoever. The long-term task will be to extend this kind of study to more sophisticated models and to create a hierarchy of plasticity models with varying degrees of accuracy for model identification of test data.

Plasticity researchers have made substantial progress in stress analysis as a boundary value problem, particularly the innovative contribution of limit analysis; however, on the other hand, in dealing with constitutive relations, they are encountered with more difficulties in much broader spectrum than they expected. Most studies of constitutive relations were concerned either with formulating models from experimental or theoretical means or both, or with devising numerical schemes to integrate constitutive equations for inclusion in large-scale software. It is felt that models are created (one by one) but not (yet) understood (fully and correctly); for example, why are initial conditions and their effects seldom discussed explicitly in such theories in terms of incremental (or rate or differential) formulations? Although they obviously constitute initial value problems when they are subjected to input paths. Hence the present paper intends to address the constitutive model issue in a somewhat distinct way; it is not an article about formulating new constitutive

[1] What "rectilinear" refers to in the present paper is precisely expressed in eqn (21). Various terminologies such as proportional, straight, linear, affine, etc., were used but their meanings might differ subtly.

* Author to whom correspondence should be addressed. Tel.: 886-2-2366-1931. Fax: 886-2-2362-2975. E-mail: msvlab@msvlab.ce.ntu.edu.tw.

models, nor is it an article of stress analysis (e.g., Kuksin, 1996). It is supposed that more carefully controlled experimentation combined with rigorous analyses of constitutive models, and global analyses of the hierarchy of constitutive models combined with the techniques of model identification and parameter estimation might contribute decisive momentum to the main stream of the studies, and that the visual sense is the most immediate we possess and helps lead directly to a better comprehension of the relatively sophisticated behavior of elastoplasticity. To pursue gradual conformity to these lines of thoughts, the present paper aims to rigorously analyze a postulated system of axioms for perfect elastoplasticity, to cultivate intuition through geometrical illustration of solutions, and to perform thorough analysis of the model for deeper understanding of the behavior by specifically subjecting the model to the input of all rectilinear generalized strain paths with all admissible initial generalized stress points.

Let the boldfaced $\mathbf{Q} = (Q_1, Q_2, \ldots, Q_n)$ and $\mathbf{q} = (q_1, q_2, \ldots, q_n)$ denote the n-vectors of generalized stresses and generalized strains, respectively, as used by Prager (1956) and many other scholars. Generalized stresses may coincide with actual stresses at a material point or with stress deviators (see Subsection 3.4), or they may be stress resultants on a cross section of a structural member like a beam, plate, or beam-column connection, etc., or they may be the restoring forces integrated at finite element nodes of a discretized continuum. Generalized strains are dual variables conjugate to the generalized stresses in a certain sense; see Prager (1959), Martin (1975), or Lubliner (1990), for example. Using these we are going to investigate in this paper the following perfect elastoplastic model:[2,3]

$$\dot{\mathbf{q}} = \dot{\mathbf{q}}^e + \dot{\mathbf{q}}^p, \tag{1}$$

$$\dot{\mathbf{Q}} = k_e \dot{\mathbf{q}}^e, \tag{2}$$

$$\mathbf{Q}\dot{q}_0 = Q_0 \dot{\mathbf{q}}^p, \tag{3}$$

$$\|\mathbf{Q}\| \leqslant Q_0, \tag{4}$$

$$\dot{\mathbf{q}}_0 \geqslant 0, \tag{5}$$

$$\|\mathbf{Q}\|\dot{q}_0 = Q_0 \dot{q}_0. \tag{6}$$

Here the norm of a vector $\mathbf{Q}$ is defined as $\|\mathbf{Q}\| := \sqrt{\mathbf{Q}\cdot\mathbf{Q}}$ and a dot between two vectors, say $\mathbf{Q}$ and $\dot{\mathbf{q}}$, denotes their inner product $\Sigma_i Q_i \dot{q}_i$. The generalized modulus of elasticity $k_e > 0$ and the generalized yield stress $Q_0 > 0$ are the only two property constants needed in the model. The boldfaced $\mathbf{q}^e$ and $\mathbf{q}^p$ are the n-vectors of generalized elastic and plastic strains, respectively, whereas q_0 is a scalar called the equivalent generalized plastic strain, with $Q_0\dot{q}_0$ being the specific power of dissipation. All $\mathbf{q}$, $\mathbf{q}^e$, $\mathbf{q}^p$, $\mathbf{Q}$ and q_0 are functions of one and the same independent variable, which in most cases is taken either as the usual time or as the arc-length of a control path; however, for convenience, the independent variable no matter what it is will be simply called "time" and given the symbol t. In the sequel, the "time" ingredient implied in such time related terms as rate, history, travel time, arrival time, spacetime, hysteresis, evolution, dynamic, temporal, long-term, isochronal, etc., should be understood likewise. An overdot denotes differentiation with respect to time, $\mathrm{d}/\mathrm{d}t$. Without loss of generality it is also postulated that with the above differential model there is a time instant designated as $t = t_0$, called the zero-value (or annealed) time, before and at which the model is in the zero-value (or annealed) state in the sense that the relevant values $\mathbf{q}(t_0)$, $\mathbf{q}^e(t_0)$, $\mathbf{q}^p(t_0)$, $\mathbf{Q}(t_0)$ and $q_0(t_0)$ are all zero.

[2] This model can be utilized to describe the Prandtl–Reuss material; see Subsection 3.4.

[3] In fact, the symbol $\dot{q}_0$ is the familiar $\dot{\lambda}$, or better $\dot{\lambda}$, in the plasticity literature. The adoption of the notation will be made clearer if one appreciates the role $(q_1, q_2, \ldots, q_n, q_0)$ plays in the $(n+1)$-dimensional Minkowski spacetime $(YQ_1, YQ_2, \ldots, YQ_n, YQ_0)$ with Y defined in eqn (9); see also eqns (8) and (13), the latter of which implies a Minkowski metric, which is diagonal with n diagonal elements $+1$ and one diagonal element -1 (Hong and Liu, 1997b).

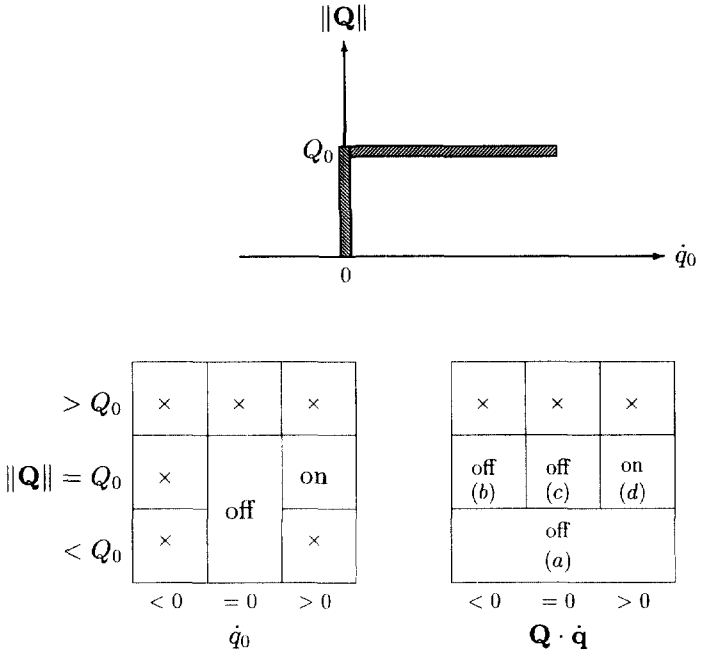

Fig. 1. The two phases (on and off) and the four cases [(a)–(d)] of the states.

It is easy to comprehend and appreciate eqns (1)–(5). Equation (3) is an associated plastic-flow rule. Equation (4) specifies admissible generalized stresses; we often call $\|\mathbf{Q}\| \leqslant Q_0$ the admissible closed ball, $\|\mathbf{Q}\| > Q_0$ the forbidden exterior, and $\|\mathbf{Q}\| = Q_0$ the yield hypersphere. Equation (5) or $Q_0\dot{q}_0 \geqslant 0$ requires the non-negativity of the power of dissipation. However, eqn (6) may need more explanation. With the aid of the two inequalities (4) and (5), it simply requires q_0 to be frozen if $\|\mathbf{Q}\| < Q_0$, so that $\dot{q}_0 = 0$ drastically reduces eqns (1)–(3) to $\dot{\mathbf{Q}} = k_e\dot{\mathbf{q}}$, an elastic relation. The significance of the complementary trios (4)–(6) cannot be overemphasized. It furnishes the model with an on-off switch for the mechanism of plasticity, and the conditions to switch on and to switch off the mechanism can thus be derived in a very precise way. Thereby the model can either be in the ON (elastoplastic) phase governed by eqns (1)–(3) or in the OFF (elastic) phase governed by $\dot{\mathbf{Q}} = k_e\dot{\mathbf{q}}$. See Fig. 1 and also refer to Subsection 2.2 for more discussions. We are reminded that the six axioms suffice for perfect elastoplasticity, so that the so-called consistency condition is merely a necessary condition in the on phase and should not be specified independently.

The reasons that we begin with so simple a model and a path may be stated below:[4] The model in the above neatly revised form is simple yet basic, retaining some most important characteristics of elastoplasticity (Hong and Liu, 1997b), and can be regarded as a prototype indicating what might be achieved by this type of modeling, rather than as definitive and conclusive statements about the real world. Also, a rectilinear path to be employed as input is too simple, but is frequently encountered in numerical calculations and experimental tests. It is known that systems are often characterized in terms of responses to elementary signals; likewise, it may be expected that in the content of mechanical properties and behavior, materials and components may be characterized phenomenologically in terms of responses to elementary paths to some extent. Moreover, attempts to make models and paths more realistic are likely to raise their complexity to a level where all but trivial issues defy solution and analysis. They being simple enough, the exact solutions can be obtained, thus making it easier to analyze them in greater depth and in a

[4]The significance of the study may be appreciated better if one notices the analogy of the mathematical structures (Hong and Liu, 1997a,b) between the perfect elastoplastic model under the rectilinear generalized strain path and the boost in special theory of relativity, which is a very important Lorentz transformation (e.g., Das, 1992; Doughty, 1990).

rigorous and exhaustive manner. Indeed, in the present paper, we attempt to go over thoroughly

(space of initial values) $\otimes$ (space of input paths)

$\otimes$(space of property constants) $\otimes$ (space of closeness)

by virtue of going over all possible values of a few control parameters[5] coined to cover the product space. Furthermore, modern mathematical tools such as those used in nonlinear dynamics and nonlinear analysis can be utilized right away. In so doing it will be observed later that the simple model and path exhibit more sophisticated behavior than usually perceived, for example, a smooth elastic–plastic transition.

The paper is divided into sections and subsections, Section 2 and Subsection 6.4 for responses to general inputs of generalized strain paths, while all the rest for responses to inputs of rectilinear generalized strain paths. Sections 3 and 6 are for the exact solutions and visualization of the solutions. Sections 4, 5 and 7 are devoted to the analysis of behavior.

2. RESPONSES AND TWO PHASES

The model is composed of two parts, namely the differential eqns (1)–(3) and the complementary trios (4)–(6). The first part can be integrated to obtain response operators (Hong and Liou, 1993). The second part with the aid of the first part creates an on-off switching mechanism of plasticity (Hong and Liu, 1993, 1997a).

2.1. *Response operator*

Substituting eqns (2) and (3) into eqn (1), we have

$$\frac{1}{k_e}\dot{\mathbf{Q}} + \frac{\dot{q}_0}{Q_0}\mathbf{Q} = \dot{\mathbf{q}}, \tag{7}$$

which becomes

$$\frac{\mathrm{d}}{\mathrm{d}t}(Y\mathbf{Q}) = k_e Y\dot{\mathbf{q}} \tag{8}$$

upon defining

$$Y := \exp\left(\frac{k_e}{Q_0}q_0\right). \tag{9}$$

The solution is

$$\mathbf{Q}(t) = \frac{Y(t_i)}{Y(t)}\mathbf{Q}(t_i) + k_e\int_{t_i}^{t}\frac{Y(\xi)}{Y(t)}\dot{\mathbf{q}}(\xi)\,\mathrm{d}\xi. \tag{10}$$

From eqns (1) and (2) we have

$$\mathbf{q}^p(t) = \mathbf{q}^p(t_i) + \frac{1}{k_e}[\mathbf{Q}(t_i) - \mathbf{Q}(t)] + \mathbf{q}(t) - \mathbf{q}(t_i). \tag{11}$$

Equation (10) defines an operator which maps generalized strain histories into generalized stress histories. Here t is the (current) time and t_i is an initial time, at which initial conditions are prescribed. We note that the initial time t_i is not necessarily the zero-value time t_0 and

[5] See Table 1 in the final section.

that the initial generalized stresses $\mathbf{Q}(t_i)$ do not necessarily vanish, for the material or component that the model represents may suffer various loadings in its earlier life before it comes into service or re-service; indeed, $t_i \geqslant t_0$, $\mathbf{Q}(t_i) \neq \mathbf{0}$ in general and $Y(t_i) \neq Y(t_0) = 1$ in general. Obviously, eqn (10) expressing that the generalized stresses can be calculated from the history of generalized strains is useful only if the history of Y [or the history of q_0 via eqn (9)] is known in advance. Thus, Y or q_0 deserves more study, as will be pursued in the following subsections.

2.2. *Plasticity switch*

The complementary trios (4)–(6) furnish the model with an on–off switch of plasticity mechanism, of which the on–off switching criterion are derived below. Taking the inner product of $\mathbf{Q}$ and the vector eqn (7), we obtain

$$\frac{1}{k_e}\mathbf{Q}\cdot\dot{\mathbf{Q}}+\frac{\dot{q}_0}{Q_0}\mathbf{Q}\cdot\mathbf{Q}=\mathbf{Q}\cdot\dot{\mathbf{q}}, \tag{12}$$

which, due to the constancy of Q_0, asserts that

$$\|\mathbf{Q}\| = Q_0 \Rightarrow \mathbf{Q}\cdot\dot{\mathbf{q}} = Q_0\dot{q}_0. \tag{13}$$

With this we readily prove the sufficiency part of the following statement:

$$\{\|\mathbf{Q}\| = Q_0 \text{ and } \mathbf{Q}\cdot\dot{\mathbf{q}} > 0\} \Leftrightarrow \{\dot{q}_0 = \mathbf{Q}\cdot\dot{\mathbf{q}}/Q_0\} \Leftrightarrow \{\dot{q}_0 > 0\}. \tag{14}$$

Conversely, if $\dot{q}_0 > 0$, eqn (6) assures $\|\mathbf{Q}\| = Q_0$, which together with eqn (13) proves the necessity part. That is, the sufficient and necessary conditions to switch on the mechanism of plasticity are the fulfillment of both the yield condition $\|\mathbf{Q}\| = Q_0$ and the straining condition $\mathbf{Q}\cdot\dot{\mathbf{q}} > 0$. Considering statement (14) and inequality (5), we discover the following on–off switching criterion for the mechanism of plasticity:

$$\dot{q}_0 = \begin{cases} \mathbf{Q}\cdot\dot{\mathbf{q}}/Q_0 > 0 & \text{iff} \quad \|\mathbf{Q}\| = Q_0 \quad \text{and} \quad \mathbf{Q}\cdot\dot{\mathbf{q}} > 0, \quad \boxed{\text{ON}} \\ 0 & \text{otherwise.} \qquad\qquad\qquad\qquad\quad \boxed{\text{OFF}} \end{cases} \tag{15}$$

From this and eqn (7) the governing equations for the model are

$$\begin{aligned} &\dot{\mathbf{Q}}+\left[\frac{k_e}{Q_0^2}\mathbf{Q}\cdot\dot{\mathbf{q}}\right]\mathbf{Q} = k_e\dot{\mathbf{q}}, \quad \boxed{\text{ON}} \\ &\dot{\mathbf{Q}} = k_e\dot{\mathbf{q}}. \qquad\qquad\qquad\qquad \boxed{\text{OFF}} \end{aligned} \tag{16}$$

To emphasize the standard structure of tangent stiffness, the above equations are rewritten as

$$\dot{\mathbf{Q}} = \begin{cases} \left[k_e\mathbf{I}-\dfrac{k_e}{Q_0^2}\mathbf{Q}\otimes\mathbf{Q}\right]\dot{\mathbf{q}}, & \boxed{\text{ON}} \\ k_e\dot{\mathbf{q}}, & \boxed{\text{OFF}} \end{cases} \tag{17}$$

where $\mathbf{I}$ is the identity and the symbol $\otimes$ denotes the tensor product.

Given k_e and Q_0, once $\mathbf{Q}$ and $\dot{\mathbf{q}}$ are known, all $\dot{\mathbf{q}}^e$, $\dot{\mathbf{q}}^p$, $\dot{\mathbf{Q}}$, $\dot{q}_0$ are readily determined according to the system of axioms (1)–(6) and the resulting criterion (15). It is, therefore, clear that the state of the model is represented by the dual pair $(\mathbf{Q}, \dot{\mathbf{q}})$, which can be categorized into four admissible cases: Case (a). The generalized stress point is inside the yield hypersphere, i.e., $\|\mathbf{Q}\| < Q_0$; Case (b). The generalized stress point is located on the

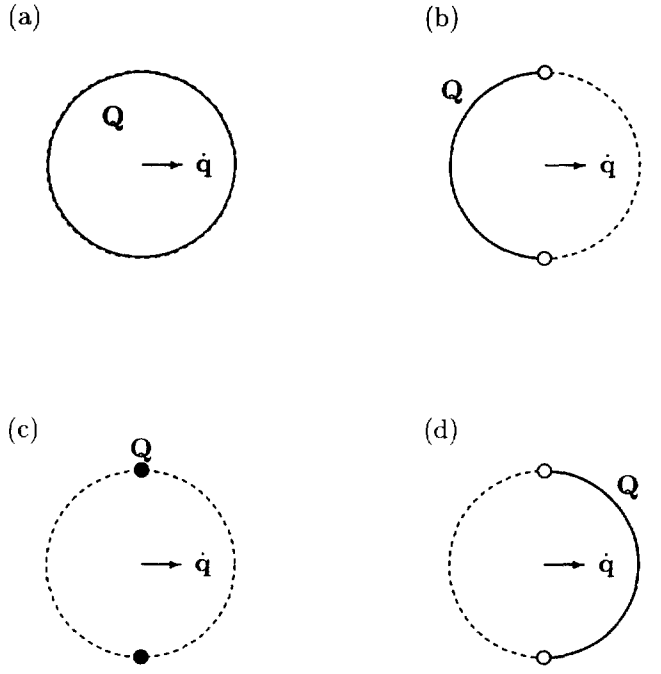

Fig. 2. Schematic diagrams for the four cases of the states represented by the generalized stress points $\mathbf{Q}$ and the generalized strain rates $\dot{\mathbf{q}}$.

yield hypersphere, i.e., $\|\mathbf{Q}\| = Q_0$, but the unstraining condition $\mathbf{Q}\cdot\dot{\mathbf{q}} < 0$ prevails; Case (c). The generalized stress point is located on the yield hypersphere, i.e., $\|\mathbf{Q}\| = Q_0$, but the neutral straining condition $\mathbf{Q}\cdot\dot{\mathbf{q}} = 0$ holds; Case (d). The generalized stress point is located on the yield hypersphere, i.e., $\|\mathbf{Q}\| = Q_0$, and the straining condition $\mathbf{Q}\cdot\dot{\mathbf{q}} > 0$ holds. According to criterion (15), the state of case (d) is in the ON (elastoplastic) phase with $\dot{q}_0 > 0$, while the ("otherwise") states of cases (a)–(c) are in the OFF (elastic) phase with $\dot{q} = 0$. Figures 1 and 2 schematically depict the four cases and the two phases.

2.3. *Plasticity measure*

The nonnegativity of $\dot{q}_0$ indicates that q_0 is a time-like parameter and plays the role of the arrow of time. From axioms (3), (5), and (6) and $Q_0 > 0$, it is not difficult to derive that

$$\dot{q}_0 = \|\dot{\mathbf{q}}^p\|, \tag{18}$$

which indicates that q_0 is the arc-length of a path in the generalized plastic strain space. According to criterion (15) and eqn (10), $q_0(t)$ determines switching-on or switching-off, sets the pace for the plasticity mechanism, and indeed serves as a measure of plastic irreversibility, the calculation of which or its homeomorphism $Y(t)$ is crucially indispensable in the evolution of the response, as has been seen in eqn (10). Based on criterion (15) and eqns (9) and (10),

$$\dot{Y}(t) = \begin{cases} \dfrac{k_e}{Q_0^2}\, Y(t_i)\mathbf{Q}(t_i)\cdot\dot{\mathbf{q}}(t) + \dfrac{k_e^2}{Q_0^2}\displaystyle\int_{t_i}^{t} \dot{\mathbf{q}}(t)\cdot\dot{\mathbf{q}}(\xi)\, Y(\xi)\, \mathrm{d}\xi, & \boxed{\text{ON}} \\ 0. & \boxed{\text{OFF}} \end{cases} \tag{19}$$

Equation $(19)_1$ is a linear Volterra integrodifferential equation of Y. Integrating and changing the order of integrations, we have

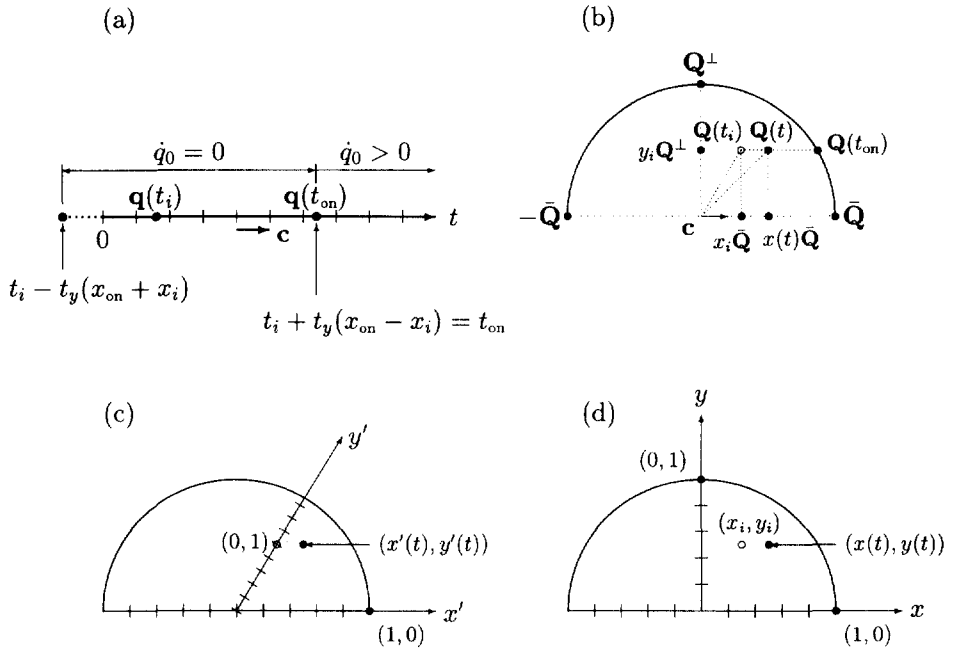

Fig. 3. Subspaces and coordinate systems. (a) Input subspace with the coordinate t with respect to the basis $\mathbf{c}$; (b) several points in response subspace; (c) coordinates (x', y') with respect to the oblique basis; (d) coordinates (x, y) with respect to the orthogonal basis.

$$Y(t) = \begin{cases} \left\{1 + \dfrac{k_e}{Q_0^2}[\mathbf{q}(t) - \mathbf{q}(t_i)] \cdot \mathbf{Q}(t_i)\right\} Y(t_i) + \dfrac{k_e^2}{Q_0^2}\displaystyle\int_{t_i}^{t} [\mathbf{q}(t) - \mathbf{q}(\xi)] \cdot \dot{\mathbf{q}}(\xi)\, Y(\xi)\, \mathrm{d}\xi, & \boxed{\text{ON}} \\ Y(t_i). & \boxed{\text{OFF}} \end{cases} \tag{20}$$

Equation $(20)_1$ is a linear Volterra integral equation of Y, amenable to further study and solution. By comparing the derivations of eqns (10) and (20), we note that although each of the two phases has its own equation for $Y(t)$, the expression (10) for $\mathbf{Q}(t)$ applies to both phases. From eqns (10) and (20), we see what really matters is $Y(t)/Y(t_i)$ rather than $Y(t)$; therefore, there is no need to worry about the initial value $Y(t_i)$. However, it is essential to specify the initial generalized stress vector $\mathbf{Q}(t_i)$ when the model is subjected to a generalized strain control, as we can see from eqn (10).

3. RESPONSES TO RECTILINEAR GENERALIZED STRAIN PATHS

Consider now a rectilinear generalized strain path specified by a nonzero constant n-vector $\mathbf{c}$, namely

$$\mathbf{q}(t) = \mathbf{q}(t_i) + (t - t_i)\mathbf{c} \tag{21}$$

with

$$\dot{\mathbf{q}} = \mathbf{c} \neq \mathbf{0}, \tag{22}$$

which is simple enough, but is frequently encountered in numerical calculations and experimental tests. It may be useful to deem that eqn (21) defines a one-dimensional input subspace of the generalized strain space with t as its coordinate, as shown in Fig. 3(a). Later on it will become clear that the initial generalized strain vector $\mathbf{q}(t_i)$ has no effects on

responses, and that, to the contrary, the initial generalized stress vector $\mathbf{Q}(t_i)$ does have significant effects on responses.

Because of the two facts that the input path prescribed by eqn (21) is characterized mainly by $\mathbf{c}$ and that the model of eqns (1)–(6), by the only two property constants k_e and Q_0, it is useful to define

$$t_y := \frac{Q_0}{k_e \|\mathbf{c}\|}. \tag{23}$$

Since Q_0/k_e is the generalized yield strain corresponding to the generalized yield stress Q_0, the t_y defined above may be called the yield time-scale—a convenient scale to non-dimensionalize time quantities so as to qualify their sizes relative to the threshold value. Notice that $t_y > 0$.

3.1. *Switch-on time*

Given the generalized strain path (21) and an initial generalized stress point $\mathbf{Q}(t_i)$ which is confined by inequality (4), if at the initial time t_i the mechanism of plasticity is not yet switched on, we want to predict in this subsection the switch-on time t_{on} at which it will be turned on. In the following a definition will be given and then a formula will be derived for the switch-on time. To facilitate the development of the whole theory in this section and the sections which follow, the definition must be precise. We caution that the less precise our thoughts are, the fuzzier our practical scientific path will be. First, we wish to designate the initial time t_i as the switch-on time t_{on} if the model at t_i is in the on phase (i.e., case (d) introduced in Subsection 2.2); moreover, we wish the definition and formula to be given apply not only to the three off-phase cases [i.e., cases (a)–(c)] but also to the on-phase case [i.e., case (d)]; and, furthermore, they apply indiscriminately to all the phases and cases such that no distinction has to be made among the four cases and between the two phases.

Definition.[6] A time instant is called a switch-on time and denoted by t_{on} if $t_b < t_{on} < t_a$ for all $t_b \in \mathring{B}_{off}$ and all $t_a \in \mathring{B}_{on}$, where $\mathring{B}_{off} = \{t | t \in \mathring{B}, \dot{q}_0(t) = 0\}$, which is allowed to be empty, and $\mathring{B}_{on} = \{t | t \in \mathring{B}, \dot{q}_0(t) > 0\}$, which should not be empty, with $\mathring{B}$ being the intersection of the punctured neighborhood of t_{on} and the time interval under consideration.

The definition emphasizes that the quintessential nature of t_{on} lies in the change of $\dot{q}_0$ between "after t_{on}" and "before t_{on}", not in the $\dot{q}_0$ at the very instant t_{on}. Define

$$x_i := \frac{\mathbf{Q}(t_i)}{Q_0} \cdot \frac{\mathbf{c}}{\|\mathbf{c}\|}, \tag{24}$$

$$y_i := \frac{\|\mathbf{Q}(t_i)\|}{Q_0} \sqrt{1 - \left(\frac{\mathbf{Q}(t_i)}{\|\mathbf{Q}(t_i)\|} \cdot \frac{\mathbf{c}}{\|\mathbf{c}\|} \right)^2}, \tag{25}$$

$$x_{on} := \sqrt{1 - y_i^2}. \tag{26}$$

Obviously $-1 \leqslant -x_{on} \leqslant x_i \leqslant x_{on} \leqslant 1$, $0 \leqslant x_{on} \leqslant 1$ and $0 \leqslant y_i \leqslant 1$.

Theorem 1. For the model (1)–(6) subjected to the path (21), the switch-on time is given by

$$t_{on} = t_i + t_y (x_{on} - x_i), \tag{27}$$

and $\dot{q}_0 > 0$ for all $t > t_{on}$ in the time interval under consideration. In other words, the control path (21) will never switch off the plasticity mechanism once it is switched on.

[6] The definition is supposed to apply to more general elastoplastic models under more general control paths, including mixed control paths. A slight modification will give the definition of the switch-off time t_{off}.

Proof: If $\dot{q}_0(t) = 0$, then the six axioms (1)–(6) reduce to the two $\dot{\mathbf{Q}}(t) = k_e\dot{\mathbf{q}}(t)$ and $\|\mathbf{Q}(t)\| \leqslant Q_0$, which are combined to

$$\mathbf{Q}(t_i)\cdot\mathbf{Q}(t_i)+2(t-t_i)k_e\mathbf{Q}(t_i)\cdot\mathbf{c}+(t-t_i)^2k_e^2\|\mathbf{c}\|^2 \leqslant Q_0^2 \tag{28}$$

for the considered control $\dot{\mathbf{q}} = \mathbf{c} \neq \mathbf{0}$. The solution is

$$t_i+t_y(-x_{on}-x_i) \leqslant t \leqslant t_i+t_y(x_{on}-x_i). \tag{29}$$

Hence $\dot{Y}(t) = 0$ [or $\dot{q}_0(t) = 0$] for t satisfying eqn (29); therefore [referring to Fig. 3(a)], if we can further prove $\dot{Y}(t) > 0$ for all $t > t_i+t_y\ (x_{on}-x_i)$, then we shall prove eqn (27) according to the definition. To this end, substituting $t_i+t_y(x_{on}-x_i)$ for t in the elastic equation $\mathbf{Q}(t) = \mathbf{Q}(t_i)+k_e(t-t_i)\mathbf{c}$, taking the inner product of the resulting equation with $\mathbf{c}$, and then using eqns (23) and (24), we obtain

$$\mathbf{Q}(t_i+t_y(x_{on}-x_i))\cdot\mathbf{c} = k_e t_y x_{on}\|\mathbf{c}\|^2 \geqslant 0, \tag{30}$$

and, using eqns $(19)_1$ and (22), we have

$$\dot{Y}(t) = \frac{k_e}{Q_0^2}\,Y(t_i+t_y(x_{on}-x_i))\mathbf{Q}(t_i+t_y(x_{on}-x_i))\cdot\mathbf{c}+\frac{k_e^2\|\mathbf{c}\|^2}{Q_0^2}\int_{t_i+t_y(x_{on}-x_i)}^{t} Y(\xi)\,\mathrm{d}\xi. \tag{31}$$

The two equations together yield $\dot{Y}(t) > 0$ strictly for all $t > t_i+t_y(x_{on}-x_i)$, so that eqn (27) is proved. For such $t > t_{on}$, we have $\dot{q}_0 = \mathbf{Q}\cdot\mathbf{c}/Q_0 > 0$ and $\|\mathbf{Q}\| = Q_0$ due to eqn (14), so that the model (1)–(6) with $\dot{\mathbf{q}} = \mathbf{c} \neq \mathbf{0}$ becomes $\dot{\mathbf{Q}}+(k_e\mathbf{Q}\cdot\mathbf{c}/Q_0^2)\mathbf{Q} = k_e\mathbf{c}$, a system of nonlinear ordinary differential equations. The existence of its solution, $\mathbf{Q}(t)$ for all $t > t_{on}$, is guaranteed by the existence theorem of the theory of ordinary differential equations.[7] The existence of such generalized stress states $\mathbf{Q}(t)$ for which $\dot{q}_0(t) > 0$ for all $t > t_{on}$ means that the control path (21) will never switch off the plasticity mechanism once the path switches the mechanism on. This completes the proof.

3.2. *Exact solution of plasticity measure*

Since for the rectilinear path (21) the plasticity mechanism is never switched off once switched on, the governing equation for the plasticity measure $Y(t)$ can be deduced from eqns (20)–(23) and Theorem 1 as

$$Y(t) = Y(t_i)+H\left(\frac{t-t_{on}}{t_y}\right)\left[x_{on}\frac{t-t_{on}}{t_y}\,Y(t_i)+\int_{t_{on}}^{t}\frac{t-\xi}{t_y}\,Y(\xi)\,\mathrm{d}\frac{\xi}{t_y}\right], \tag{32}$$

where H is the (Heaviside) unit step function with $H(\xi) = 0$ if $\xi < 0$, $H(\xi) = 1$ if $\xi > 0$ and $H(0)\in[0,1]$.[8] According to the definition adopted, $H(\xi)$ is maximal monotone and is multiple-valued at $\xi = 0$. Indeed, the definition further renders, as to be made clear later in Subsection 6.2, $\dot{Y}(t)$ and $\dot{q}_0(t)$ to be maximal monotone increasing, and multiple-valued at $t = t_{on}$.[9] The exact solution of the integral eqn (32) is

$$Y(t) = Y(t_i)[1-H_1(t)+H_c(t)+x_{on}H_s(t)], \tag{33}$$

where

[7] See, for example, Hirsch and Smale (1974).

[8] The definition is consistent with the concept of multiplicity of plastic flow vectors at a corner of yield surface in the theory of plasticity and also with the definition of subdifferentiability in the theory of convex analysis and monotone operators.

[9] For the rare, extreme case (c) mentioned in Subsection 2.2, $\dot{q}_0(t_{on}) = 0$; that is, the multiple-valuedness of $\dot{q}_0(t_{on})$ degenerates into single-valuedness for case (c).

$$H_1(t) := H\left(\frac{t-t_{on}}{t_y}\right),$$

$$H_c(t) := H\left(\frac{t-t_{on}}{t_y}\right)\cosh\frac{t-t_{on}}{t_y},$$

$$H_s(t) := H\left(\frac{t-t_{on}}{t_y}\right)\sinh\frac{t-t_{on}}{t_y}. \tag{34}$$

Once $Y(t)$ is available through eqn (33), $q_0(t)$ can be calculated via eqn (9). Note that the homeomorphisms $Y(t)$ and $q_0(t)$ obtained herein are continuous (and single-valued) all the way.

3.3. *Exact solution of generalized stresses*

Substituting eqns (22) and (33) and

$$\int_{t_i}^{t} Y(\xi)\,d\xi = Y(t_i)\{(t-t_i)[1-H_1(t)]+t_y[-x_iH_1(t)+x_{on}H_c(t)+H_s(t)]\} \tag{35}$$

into eqn (10), we have

$$\mathbf{Q}(t) = \frac{1}{1-H_1(t)+H_c(t)+x_{on}H_s(t)}\mathbf{Q}(t_i) + \frac{\frac{t-t_i}{t_y}[1-H_1(t)]-x_iH_1(t)+x_{on}H_c(t)+H_s(t)}{1-H_1(t)+H_c(t)+x_{on}H_s(t)}\bar{\mathbf{Q}}, \tag{36}$$

which supplies a nonlinear mapping from $\mathbf{Q}(t_i)$ to $\mathbf{Q}(t)$ for all $t \geqslant t_i$, with

$$\bar{\mathbf{Q}} := \frac{Q_0\mathbf{c}}{\|\mathbf{c}\|}. \tag{37}$$

The expression indicates that the generalized stress response is dependent upon the initial generalized stress vector $\mathbf{Q}(t_i)$, the generalized strain rate vector $\mathbf{c}$, and the property constants k_e and Q_0, but is not affected by the initial values $\mathbf{q}(t_i)$ (or $\mathbf{q}^e(t_i)$ and $\mathbf{q}^p(t_i)$) and $q_0(t_i)$ [or $Y(t_i)$]. The influence of prestress $\mathbf{Q}(t_i)$ will be elaborated in Section 5 and Subsection 7.2, and the effect of the direction $\mathbf{c}/\|\mathbf{c}\|$ will be explored in Subsection 6.3, while the size $\|\mathbf{c}\|$ and the properties k_e and Q_0 are grouped into one parameter t_y, the yield time-scale defined in eqn (23), which as can be seen has significant influence throughout.

3.4. *An application to numerical integration of a material model*

In the vast literature of numerical plasticity a great effort was made to devise numerical integration schemes for elastoplastic materials; for instance, in Krieg and Krieg (1977) the material dealt with was the Prandtl–Reuss model and the control paths considered were rectilinear strain paths. In fact, under that model and those paths, the preceding subsections provide the exact solutions if we take[10,11]

$$n = 9,$$

$$\mathbf{Q} = (s_{11}, s_{22}, s_{33}, s_{23}, s_{13}, s_{12}, s_{21}, s_{31}, s_{32}), \quad Q_0 = \sqrt{2}h,$$

$$\mathbf{q} = (e_{11}, e_{22}, e_{33}, e_{23}, e_{13}, e_{12}, e_{21}, e_{31}, e_{32}), \quad q_0 = \bar{\gamma}^p/\sqrt{2},$$

$$k_e = 2G,$$

[10] The realization is not unique.

[11] The numerical coefficients before $\bar{\gamma}^p$ and h will change if the definitions of $\bar{\gamma}^p$ and h change, and moreover, the two numbers are mutually dependent.

where s_{ij} = the ij component of the symmetric Cartesian tensor of stress deviator, e_{ij} = the ij component of the symmetric Cartesian tensor of strain deviator, h = yield stress in shearing, $\bar{\gamma}^p$ = equivalent shear plastic (engineering) strain, G = shear modulus of elasticity.

The above deviatoric part must be supplemented by the following volumetric part:

$$\sigma_{kk}(t) = \sigma_{kk}(t_i) + 3K[\varepsilon_{ll}(t) - \varepsilon_{ll}(t_i)],$$

where the summation convention for repeated indices has been used and σ_{ij} = the ij component of the symmetric Cartesian tensor of stress, ε_{ij} = the ij component of the symmetric Cartesian tensor of strain, K = bulk modulus of elasticity.

By now the problems posed in the cited reference have all been solved exactly; however, for the Prandtl–Reuss material subjected to rectilinear strain paths there are much more than can be said; we will present them (although in terms of generalized stresses and strains) in the sections which follow.

4. STRENGTH AND STABILITY

In this section, in order to enhance our understanding of the model behavior, we perform a dynamic theoretic study,[12] examining the evolution of the responses, especially the long-term behavior, and the stability of the model subjected to the rectilinear generalized strain paths (21) with various initial generalized stress points.

4.1. *Limit strength vector*

In this subsection we explore the long-term behavior. First, we take the limit of the $(n+1)$-vector $(\mathbf{Q}, \dot{q}_0)$ to explore the issue of limit point. Taking the limit in both sides of eqn (36) and noting Theorem 1 and eqn (34), we readily have

$$\lim_{t\to\infty} \mathbf{Q} = \bar{\mathbf{Q}}. \tag{38}$$

Hence $\bar{\mathbf{Q}}$ defined in eqn (37) is just the limit strength vector for the generalized stress response. It is easy to check

$$\lim_{t\to\infty} \|\mathbf{Q}(t)\| = Q_0. \tag{39}$$

From eqns (13), (22), (37) and (38) we have

$$\lim_{t\to\infty} \dot{q}_0 = \frac{1}{Q_0} \lim_{t\to\infty} \mathbf{Q}\cdot\mathbf{c} = \|\mathbf{c}\|. \tag{40}$$

Since the limit exists, define

$$\bar{\dot{q}}_0 := \lim_{t\to\infty} \dot{q}_0 = \|\mathbf{c}\|. \tag{41}$$

This is the limit power of dissipation.

Next, we look after the limit of $(\dot{\mathbf{Q}}, \ddot{q}_0)$ to explore the issue of a fixed point. Taking the limit in both sides of eqn (7) and noting eqns (22), (40), (38) and (37), we have

[12] The term "dynamic theoretic" used herein refers to the theory of nonlinear dynamics. It is neither related to the inertia effect, nor is it necessarily the physical time. It plainly emphasizes changing, evolving, and the like, with respect to some convenient scale—the independent variable of the model. Recalling the independent variable of our model is, as earlier stated in Section 1, the usual time or the arc-length of the control path, or even others, and is for convenience given the generic name "time" and the generic symbol t.

$$\lim_{t\to\infty}\dot{\mathbf{Q}} = k_c \lim_{t\to\infty}\left[\dot{\mathbf{q}} - \frac{\dot{q}_0}{Q_0}\mathbf{Q}\right] = 0, \tag{42}$$

which asserts that the limit strength vector $\bar{\mathbf{Q}}$ is a fixed point, since at this point it is no longer changing with the time. From eqns (13), (22) and (42),

$$\lim_{t\to\infty}\ddot{q}_0 = \frac{1}{Q_0}\lim_{t\to\infty}\dot{\mathbf{Q}}\cdot\mathbf{c} = 0, \tag{43}$$

so that we confirm the limit $\bar{\dot{q}}_0$ of $\dot{q}_0$ is a fixed value. In summary, we have shown that although the paths of the $[\mathbf{Q}(t), \dot{q}_0(t)]$ responses to the input paths (21) with the same $\mathbf{c}$ are different with different initial $[\mathbf{Q}(t_i), \dot{q}_0(t_i)]$ points, they tend to the same limit and fixed point $(\bar{\mathbf{Q}}, \bar{\dot{q}}_0)$ irrespective of different initial $[\mathbf{Q}(t_i), \dot{q}_0(t_i)]$ points. Hence $(\bar{\mathbf{Q}}, \bar{\dot{q}}_0)$ is a point attractor of the space $(\mathbf{Q}, \dot{q}_0)$. As $t \to \infty$, the $(n+1)$-vectors $(\mathbf{Q}, Q_0) \to (\bar{\mathbf{Q}}, Q_0)$ and $(\dot{\mathbf{q}}, \dot{q}_0) \to (\mathbf{c}, \bar{\dot{q}}_0)$, where Q_0 and $\mathbf{c}$ are constant. Moreover, $(\bar{\mathbf{Q}}, Q_0)$ is proportional to $(\mathbf{c}, \bar{\dot{q}}_0)$, because $(\bar{\mathbf{Q}}, Q_0) = (\mathbf{c}, \bar{\dot{q}}_0)Q_0/\|\mathbf{c}\|$.[13]

4.2. *Stability theorem by Lyapunov's direct method*

The study of the point attractor in the foregoing subsection was based mainly on the exact solution (36); in the sequel we base the study directly on the governing differential equations. Respectively, from eqns (7) and (22) and from eqns (9), (32) and (22), we have

$$\frac{\mathrm{d}}{\mathrm{d}t}\mathbf{Q} = k_c\mathbf{c} - \frac{k_c\dot{q}_0}{Q_0}\mathbf{Q}, \tag{44}$$

$$\frac{\mathrm{d}}{\mathrm{d}t}\dot{q}_0 = \frac{k_c}{Q_0}[\|\mathbf{c}\|^2 H_1(t) - (\dot{q}_0)^2], \tag{45}$$

which together compose a system of first-order differential equations for $(\mathbf{Q}, \dot{q}_0)$. Recall that in the literature of nonlinear dynamics a fixed point of a dynamic (flow) system $\dot{\mathbf{x}} = \mathbf{f}(\mathbf{x}, t)$ is characterized by $\dot{\mathbf{x}} = \mathbf{f} = \mathbf{0}$ (e.g., Smale, 1967; Thompson and Stewart, 1993). Thus, by nullifying the terms on the right-hand sides of eqns (44) and (45) and taking positive roots of the resulting system of algebraic equations to conform to axiom (5), the fixed point is obtained as follows:

$$\bar{\mathbf{Q}} = \frac{Q_0}{\|\mathbf{c}\|}\mathbf{c}, \quad \bar{\dot{q}}_0 = \|\mathbf{c}\|, \tag{46}$$

the former of which is just the one given in eqn (37). From eqns (15), (4) and (22) we have

$$0 \leqslant \dot{q}_0 \leqslant \|\mathbf{c}\|. \tag{47}$$

By eqn $(46)_2$,

$$\dot{q}_0 \leqslant \bar{\dot{q}}_0. \tag{48}$$

Due to inequality (47), we deduce from eqn (45):

$$\ddot{q}_0 \geqslant 0, \tag{49}$$

the equality of which holds if $\dot{q}_0 = \bar{\dot{q}}_0$. Hence

[13] Although they are proportional, the null $(n+1)$-vectors $(\bar{\mathbf{Q}}, Q_0)$ and $(\mathbf{c}, \bar{\dot{q}}_0)$ are M-orthogonal, namely orthogonal in the Minkowski sense, which seems counterintuitive (Hong and Liu, 1997b).

$$\frac{(\dot{q}_0-\bar{\dot{q}}_0)\ddot{q}_0}{(\bar{\dot{q}}_0)^2}\leqslant 0, \tag{50}$$

the equality of which holds if $\dot{q}_0=\bar{\dot{q}}_0$. Using eqns (36) and (44) we can prove

$$\frac{(\mathbf{Q}-\bar{\mathbf{Q}})\cdot\dot{\mathbf{Q}}}{Q_0^2}\leqslant 0, \tag{51}$$

the equality of which holds if and only if $\mathbf{Q}=\bar{\mathbf{Q}}$.

Now introduce the strict Lyapunov function:[14]

$$V=V(\mathbf{Q},\dot{q}_0):=\frac{\|\mathbf{Q}-\bar{\mathbf{Q}}\|^2}{\|\bar{\mathbf{Q}}\|^2}+\frac{(\dot{q}_0-\bar{\dot{q}}_0)^2}{2(\bar{\dot{q}}_0)^2}. \tag{52}$$

Its time derivative is

$$\dot{V}=\frac{(\mathbf{Q}-\bar{\mathbf{Q}})\cdot\dot{\mathbf{Q}}}{Q_0^2}+\frac{(\dot{q}_0-\bar{\dot{q}}_0)\ddot{q}_0}{(\bar{\dot{q}}_0)^2}. \tag{53}$$

So according to Lyapunov's stability theorem,[15] upon considering the two inequalities (51) and (50) with the two comments which just follow them, the following theorem can be drawn:

Theorem 2. The fixed point $(\bar{\mathbf{Q}},\bar{\dot{q}}_0)$ is asymptotically stable, i.e.,

(a) $V=0$ if $(\mathbf{Q},\dot{q}_0)=(\bar{\mathbf{Q}},\bar{\dot{q}}_0)$ and $V>0$ if $(\mathbf{Q},\dot{q}_0)\neq(\bar{\mathbf{Q}},\bar{\dot{q}}_0)$,

(b) $\dot{V}=0$ if $(\mathbf{Q},\dot{q}_0)=(\bar{\mathbf{Q}},\bar{\dot{q}}_0)$ and $\dot{V}<0$ if $(\mathbf{Q},\dot{q}_0)\neq(\bar{\mathbf{Q}},\bar{\dot{q}}_0)$.

In other words, the fixed point $(\bar{\mathbf{Q}},\bar{\dot{q}}_0)$ is a point attractor of the space $(\mathbf{Q},\dot{q}_0)$.

Figure 4 demonstrates three examples of the responses $(\mathbf{Q},\dot{q}_0,\ddot{q}_0)$ to the same input of generalized strain path but with three different initial generalized stress points—one zero vector and the other two nonzero. It can be seen in Fig. 4(c) that the limit strength vector $\bar{\mathbf{Q}}$ is asymptotically stable in the generalized stress space. For the first example, path 1, the heavy lines in Fig. 4(a)–(c) show that, once switched on, the generalized stress components Q_1 and Q_2 are not varying again, that is to say the point $\bar{\mathbf{Q}}/Q_0=(\bar{Q}_1,\bar{Q}_2)/Q_0=(\sqrt{2}/2,-\sqrt{2}/2)$ is a fixed point. However, for the other two examples, displayed in the lines fitted with black circles and the lines fitted with blank squares, the generalized stress paths essentially tend to that point very fast, and they are as closer to the point as the time elapses, but in fact it will take an infinite time to arrive at that point, so that in this sense the limit strength vector $\bar{\mathbf{Q}}$ is a limit point.

We will return back to the three examples of Fig. 4 in Subsection 6.2 to study their dynamics of dissipation. In the next section we will construct and classify generalized stress–strain curves.

5. GENERALIZED STRESS–STRAIN CURVES

If the generalized strain rate component $c_l\neq 0$, we can construct from eqns (21), (23) and (36) the curve of the generalized stress component Q_k vs the generalized strain component q_l corresponding to c_l as follows:

[14] See, for example, Lyapunov (1992).
[15] See, for example, Hirsch and Smale (1974).

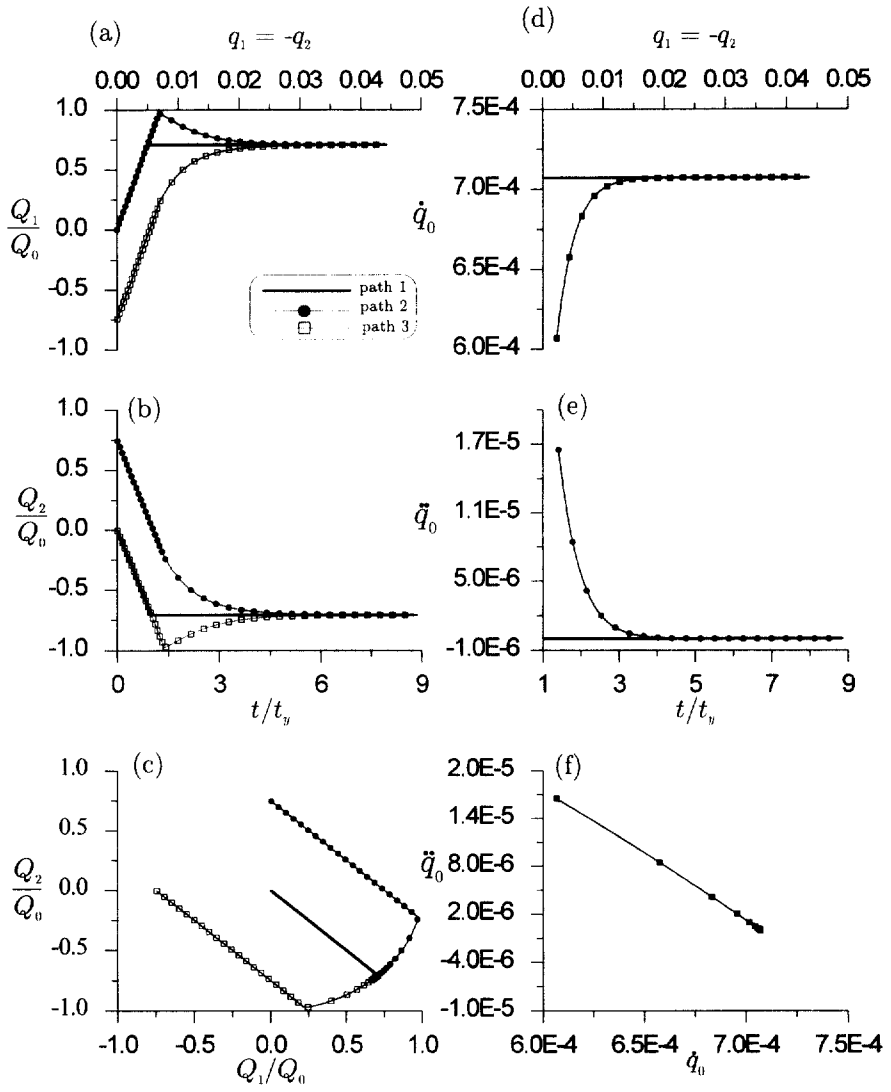

Fig. 4. Responses of the perfect elastoplastic model with three different initial generalized stress points but under the same generalized strain rate. (a) Q_1 vs t, q_1 and q_2; (b) Q_2 vs t, q_2 and q_1; (c) generalized stress paths; (d) $\dot{q}_0$ vs t, q_1 and q_2; (e) $\ddot{q}_0$ vs t, q_1 and q_2; (f) paths of $(\dot{q}_0, \ddot{q}_0)$.

$$Q_k = f_{kl}(q_l)$$

$$:= \frac{Q_k(t_i) + k_e c_k \left\{ \dfrac{q_l - q_l(t_i)}{c_l} [1 - H_1(t)] + t_y [-x_i H_1(t) + x_{on} H_c(t) + H_s(t)] \right\}}{1 - H_1(t) + H_c(t) + x_{on} H_s(t)},$$

$$\text{with } t = t_i + \frac{q_l - q_l(t_i)}{c_l}, \quad l \text{ no sum}, \quad \text{and} \quad k, l = 1, 2, \ldots, n. \tag{54}$$

It is evident from the equation that for a fixed number k the n curves of Q_k vs q_l, $l = 1, 2, \ldots, n$, are of the same geometrical shapes. We observe that the perfect elastoplastic model can exhibit a rather smooth generalized stress–strain curve, as manifested in the curves of Q_1 vs q_1 and Q_1 vs q_2 for path 3 in Fig. 4(a) and the curves of Q_2 vs q_2 and Q_2 vs q_1 for path 2 in Fig. 4(b), and a curve of the peak-residual-strength type as manifested in the curves of Q_1 vs q_1 and Q_1 vs q_2 for path 2 in Fig. 4(a) and the curves of Q_2 vs q_2 and Q_2 vs q_1 for path 3 in Fig. 4(b). It is interesting to distinguish that the component Q_1 of example

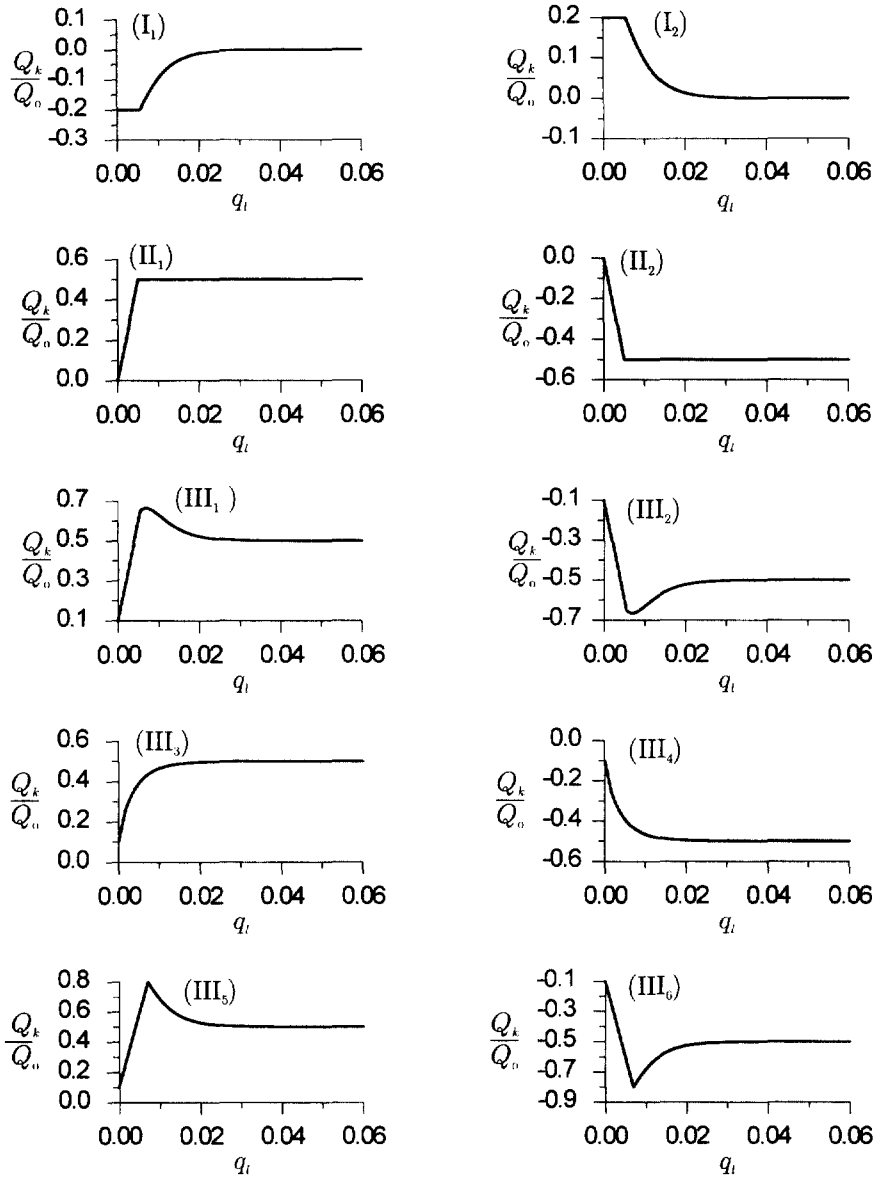

Fig. 5. Generalized stress–strain curves of perfect elastoplastic model under rectilinear generalized strain paths. There are totally ten types of shapes.

2, path 2, does not change monotonically, but in example 3, path 3, it is the component Q_2 which does not change monotonically.

How many types of geometrical shapes of curves are described by eqn (54)? In order to answer the question we need to consider three cases, namely (I) $c_k = 0$ and $0 \leqslant x_{on} \leqslant 1$, (II) $c_k \neq 0$ and $x_{on} = 1$, and (III) $c_k \neq 0$ and $0 \leqslant x_{on} < 1$. For case (I), eqn (54) reduces to

$$Q_k = \frac{Q_k(t_i)}{1 - H_1(t) + H_c(t) + x_{on} H_s(t)}. \tag{55}$$

Depending on the sign of $Q_k(t_i)$, the equation depicts two types of generalized stress–strain curves as shown in Fig. 5(I_1) for $Q_k(t_i) < 0$ and Fig. 5 (I_2) for $Q_k(t_i) > 0$. These two curves display the relaxation of generalized stress; in fact, they relax to zero stress.

Next, for case (II) we have $y_i = 0$ via eqn (26); thus, $\mathbf{Q}(t_i) = x_i Q_0 \mathbf{c}/\|\mathbf{c}\|$, $-1 \leqslant x_i \leqslant 1$ by eqn (25). Under these conditions, noting that $Q_k(t_i) - k_e c_k t_y x_i = 0$, we obtain from eqn (54) that

$$Q_k = \left[Q_k(t_i) + k_e c_k \frac{q_l - q_l(t_i)}{c_l} \right] [1 - H_1(t)] + k_e c_k t_y H_1(t). \tag{56}$$

Similarly, depending on the sign of c_k, there are two types of generalized stress–strain curves for this case, as shown in Fig. 5(II_1) for $c_k > 0$ and Fig. 5(II_2) for $c_k < 0$. These two curves display the plastic plateau of generalized stress after switching on. For this case the ultimate strengths of the curves are $Q_0 c_k/\|\mathbf{c}\|$.

Case (III) is much more complicated than the previous two cases. The detailed analyses and derivations are given in the Appendix. It is found that the three parameters $Q_k(t_i)/(k_e c_k t_y)$, x_i and x_{on} play the key role in shaping the geometrical forms of generalized stress–strain curves. As a result, case (III) has three types of curves for $c_k > 0$ and also three types of curves for $c_k < 0$; therefore, for this case there exist totally six types of generalized stress–strain curves as shown in Fig. 5(III_1)–(III_6). The residual strengths of the six curves are all $Q_0 c_k/\|\mathbf{c}\|$ as before, but the peak or ultimate strengths may be different. For curves (III_2) and (III_5) the ultimate strengths are just the residual strengths; for curves (III_3) and (III_6) the peak strengths are $Q_k(t_{\mathrm{on}}) = Q_k(t_i) + k_e c_k t_y (x_{\mathrm{on}} - x_i)$; finally, for curves ($\mathrm{III}_1$) and ($\mathrm{III}_4$) the peak strengths occur at $t = t_s$ as defined in eqn (A13). Substituting eqn (A13) into eqn (54) we obtain the peak strength

$$Q_k(t_s) = k_e c_k t_y \frac{1 - x_{\mathrm{on}}^2 + \sqrt{[1 - x_{\mathrm{on}}^2]^2 + \left(\dfrac{Q_k(t_i)}{k_e c_k t_y} - x_i \right)^2 (1 - x_{\mathrm{on}}^2)} + \dfrac{Q_k(t_i)}{k_e c_k t_y} \left(\dfrac{Q_k(t_i)}{k_e c_k t_y} - x_i \right)}{1 - x_{\mathrm{on}}^2 + \sqrt{[1 - x_{\mathrm{on}}^2]^2 + \left(\dfrac{Q_k(t_i)}{k_e c_k t_y} - x_i \right)^2 (1 - x_{\mathrm{on}}^2)}}. \tag{57}$$

Let us now go further to investigate how the six types of curves are distributed in the three-dimensional space of the aforementioned three parameters? Either $c_k > 0$ or $c_k < 0$, there are three regions in the parametric space: $\dot{Q}_k(t_{\mathrm{on}}) > 0$, $\dot{Q}_k(t_{\mathrm{on}}) < 0$ and $\dot{Q}_k(t_s) = 0$. The curve (III_1) [resp. (III_4)] which has a zero slope [i.e., a smooth peak (resp. trough)] at t_s corresponds to a point in the region $\dot{Q}_k(t_s) = 0$ and $c_k > 0$ (resp. $c_k < 0$), which is present in the sections of constant values of $Q_k(t_i)/(k_e c_k t_y) > x_i$ but disappears in the sections of $Q_k(t_i)/(k_e c_k t_y) \leqslant x_i$, as indicated by eqn (A12). The monotonic curve (III_2) [resp. (III_5)] corresponds to a point in the region $\dot{Q}_k(t_{\mathrm{on}}) > 0$ [resp. $\dot{Q}_k(t_{\mathrm{on}}) < 0$] in the parametric space for $c_k > 0$ (resp. $c_k < 0$). The curve (III_3) [resp. (III_6)] which has a sharp peak (resp. trough) corresponds to a point in the region $\dot{Q}_k(t_{\mathrm{on}}) < 0$ [resp. $\dot{Q}_k(t_{\mathrm{on}}) > 0$] in the parametric space for $c_k > 0$ (resp. $c_k < 0$). For demonstration, Fig. 6 displays a section $Q_k(t_i)/(k_e c_k t_y) = 0.2$ in the three-dimensional parametric space. Fig. 6(a) showing the regions of $\dot{Q}_k(t_{\mathrm{on}}) > 0$, $\dot{Q}_k(t_{\mathrm{on}}) < 0$ and $\dot{Q}_k(t_s) = 0$ for the case $c_k > 0$ and Fig. 6(b) showing the three regions for the case $c_k < 0$.

6. GEOMETRIC THINKING

In this section we attempt to achieve a more intuitive understanding of the input–output relationship of perfect elastoplasticity. After digesting the results of the foregoing sections, we further develop geometric constructions.

6.1. *Response subspace*

Equation (36) indicates the generalized stress response always lies in the subspace spanned by $\bar{\mathbf{Q}}$ and $\mathbf{Q}(t_i)$, which is two-dimensional if $\mathbf{Q}(t_i)$ and $\mathbf{c}$ are linearly independent, but

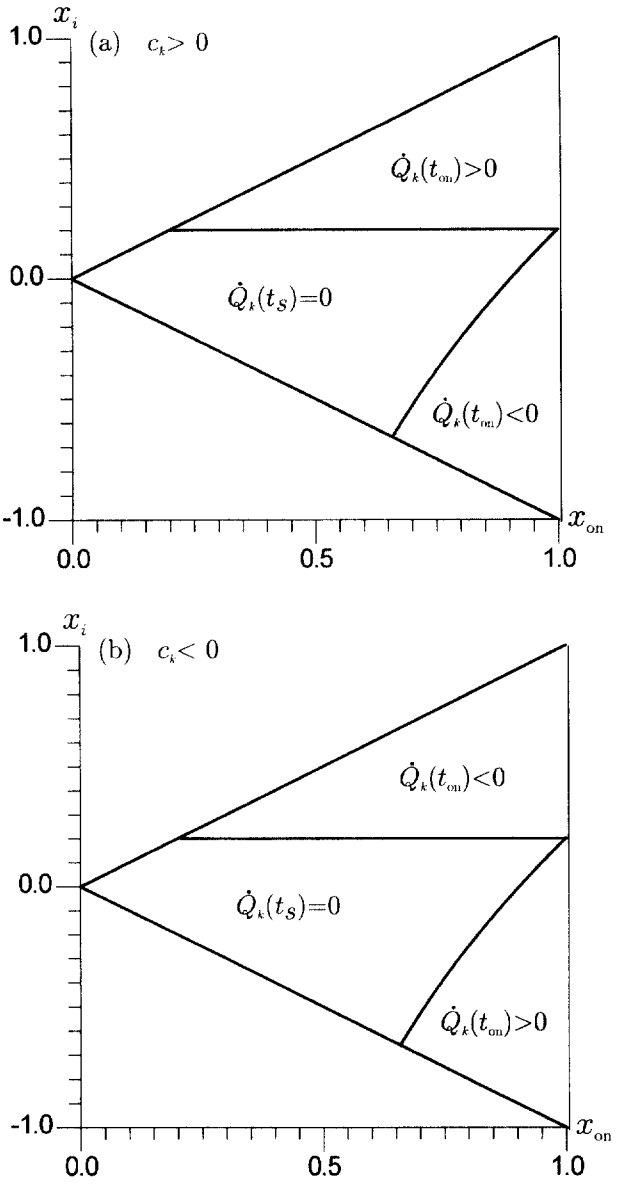

Fig. 6. The parametric plane (x_{on}, x_i) for the six types of generalized stress–strain curves for case (III). The regions of $\dot{Q}_k(t_i) = 0$, $\dot{Q}_k(t_{on}) > 0$ and $\dot{Q}_k(t_{on}) < 0$ for (a) $c_k > 0$ and (b) $c_k < 0$. The plot shown was produced for a particular section $Q_k(t_i)/(k_c c_k t_y) = 0.2$ in the three-dimensional parametric space.

degenerates into one-dimensional in case $\bar{\mathbf{Q}}$ and $\mathbf{Q}(t_i)$ are linearly dependent. Geometrically speaking, the admissible closed ball $\|\mathbf{Q}\| \leqslant Q_0$ and its boundary, the yield hypersphere $\|\mathbf{Q}\| = Q_0$, are both centered at the origin $\mathbf{Q} = \mathbf{0}$ of the generalized stress space; the generalized strain rate vector $\mathbf{c}$ furnishes the yield hypersphere a directed axis and a limit strength vector $\bar{\mathbf{Q}}$; and the response subspace is a hyperplane containing the directed axis, passing through the three points: the center, the limit strength point and the initial point, and cutting the yield hypersphere at a great circle. The response path is either composed of a straight line-segment in Euclidean n-space $\mathbb{E}^n$ followed by a great circular arc on the $(n-1)$-sphere $\mathbb{S}^{n-1}$, or simply a great circular arc on $\mathbb{S}^{n-1}$ alone. In other words, it follows the "shortest, straightest" admissible track, or in the language of geometry a geodesic in the n-dimensional closed ball $\mathbb{B}^n$. The straight line-segment is parallel to the directed axis and starts at the initial point $\mathbf{Q}(t_i)$ and ends at the switch-on point $\mathbf{Q}(t_{on})$. Being part of the great circle, the great circular arc starts either at the switch-on point $\mathbf{Q}(t_{on})$ or at the initial

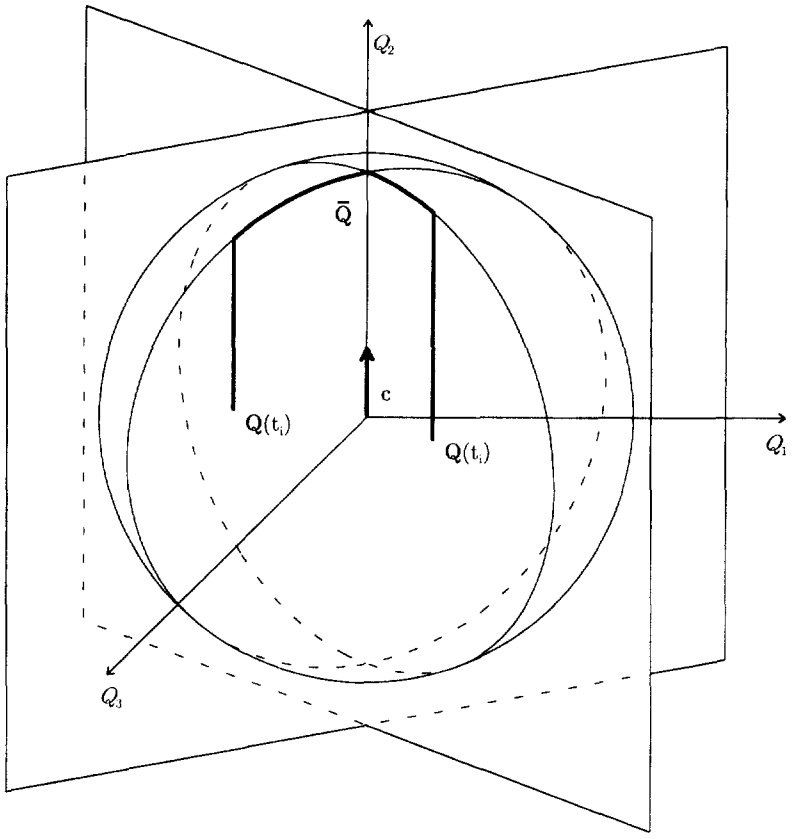

Fig. 7. Schematic plot of the two response subspaces for two different initial generalized stress points but with the same limit strength point $\bar{\mathbf{Q}}$.

point $\mathbf{Q}(t_i)$ which is already in the on phase. If fixing $\mathbf{c}$ but varying $\mathbf{Q}(t_i)$, the yield hypersphere has a fixed directed axis and a fixed north pole $\bar{\mathbf{Q}}$ but perhaps more than one response hyperplanes intersecting at the fixed directed axis. At each $\mathbf{Q}(t_i)$ starts one response path; although coming differently every path goes to the same limit point $\bar{\mathbf{Q}}$. Plotted in Fig. 7 are two response subspaces erected by two different initial generalized stress points but with the same generalized strain rate vector $\mathbf{c}$, the limit strength vector being indicated by $\bar{\mathbf{Q}}$.

Let us define

$$\mathbf{Q}^{\perp} := \left(\mathbf{Q} - \frac{\mathbf{Q}\cdot\mathbf{c}}{\|\mathbf{c}\|}\frac{\mathbf{c}}{\|\mathbf{c}\|}\right) \Big/ \sqrt{\left(\frac{\|\mathbf{Q}\|}{Q_0}\right)^2 - \left(\frac{\mathbf{Q}}{Q_0}\cdot\frac{\mathbf{c}}{\|\mathbf{c}\|}\right)^2} \tag{58}$$

and, upon substituting eqn (36) into the above definition formula, observe $\mathbf{Q}^{\perp}(t) = \mathbf{Q}^{\perp}(t_i)$ for all $t \geqslant t_i$, that is, the $\mathbf{Q}^{\perp}$ so defined is fixed. We further observe that $\bar{\mathbf{Q}}$ and $\mathbf{Q}^{\perp}$ constitute an orthogonal basis for the response subspace since $\mathbf{Q}^{\perp} \perp \bar{\mathbf{Q}}$ and $\|\bar{\mathbf{Q}}\| = \|\mathbf{Q}^{\perp}\| = Q_0$, whereas $\bar{\mathbf{Q}}$ and $\mathbf{Q}(t_i)$ form an oblique basis. Introduce two generalized coordinates x and y with respect to the orthogonal basis such that

$$\mathbf{Q}(t) = x(t)\bar{\mathbf{Q}} + y(t)\mathbf{Q}^{\perp}, \tag{59}$$

where

$$x(t) := \frac{\mathbf{Q}(t)}{Q_0} \cdot \frac{\mathbf{c}}{\|\mathbf{c}\|}, \tag{60}$$

$$y(t) := \frac{\|\mathbf{Q}(t)\|}{Q_0} \sqrt{1 - \left(\frac{\mathbf{Q}(t)}{\|\mathbf{Q}(t)\|} \cdot \frac{\mathbf{c}}{\|\mathbf{c}\|} \right)^2}. \tag{61}$$

Definitions (60) and (61) if evaluated at the initial time t_i match definitions (24) and (25), namely $x_i = x(t_i)$ and $y_i = y(t_i)$. Thus the response path (36) expressed with respect to the oblique basis can now be expressed with respect to the orthogonal basis as

$$\mathbf{Q}(t) = \frac{\left[x_i + \dfrac{t - t_i}{t_y} \right][1 - H_1(t)] + x_{\text{on}} H_c(t) + H_s(t)}{1 - H_1(t) + H_c(t) + x_{\text{on}} H_s(t)} \bar{\mathbf{Q}} + \frac{y_i}{1 - H_1(t) + H_c(t) + x_{\text{on}} H_s(t)} \mathbf{Q}^{\perp}. \tag{62}$$

Comparison of eqn (59) with eqn (62) gives the formulae for $x(t)$ and $y(t)$. Similarly, comparison of $\mathbf{Q}(t) = x'(t)\bar{\mathbf{Q}} + y'(t)\mathbf{Q}(t_i)$ with eqn (36) gives the formulae for $x'(t)$ and $y'(t)$. Thus we have established a two-dimensional response subspace and two coordinate systems (x, y) and (x', y') on it. In fact, we have already had a one-dimensional input subspace and a coordinate system (t) on it. The mapping $t \mapsto (x, y)$ or $t \mapsto (x', y')$ gives the response path and describes the input–output relationship to some extent.

Figure 3 displays the input and response subspaces, the coordinate systems, the positions of the initial generalized strain point $\mathbf{q}(t_i)$ and the current generalized strain point $\mathbf{q}(t)$ in the input subspace, in which $\mathbf{q}(t_i)$ and $\mathbf{q}(t)$ have the coordinates (t_i) and (t), respectively, with respect to the basis $\mathbf{c}$ as shown in Fig. 3(a), and the positions of the initial generalized stress point $\mathbf{Q}(t_i)$, the current generalized stress point $\mathbf{Q}(t)$, the limit strength vector (or the north pole) $\bar{\mathbf{Q}}$, the south pole $-\bar{\mathbf{Q}}$, the orthogonal point $\mathbf{Q}^{\perp}$, the switch-on point $\mathbf{Q}(t_{\text{on}})$, etc., in the response subspace, in which $\mathbf{Q}(t_i)$, $\mathbf{Q}(t)$, $\bar{\mathbf{Q}}$ have the coordinates $(0, 1)$, $(x'(t), y'(t))$, $(1, 0)$ with respect to the oblique basis $(\bar{\mathbf{Q}}, \mathbf{Q}(t_i))$ as shown in Fig. 3(c) but have the coordinates (x_i, y_i), $(x(t), y(t))$, $(1, 0)$ with respect to the orthogonal basis $(\bar{\mathbf{Q}}, \mathbf{Q}^{\perp})$ as shown in Fig. 3(d). It is easy to check $0 \leqslant (\|\mathbf{Q}\|/Q_0)^2 = x^2 + y^2 \leqslant 1$, $-1 \leqslant x_i \leqslant x(t) \leqslant 1$, $0 \leqslant y(t) \leqslant y_i \leqslant 1$ and $\dot{x}(t) \geqslant 0$, $\dot{y}(t) \leqslant 0$.

6.2. *Dissipation*

The specific work dissipated is $Q_0 q_0$; the specific power of dissipation is $Q_0 \dot{q}_0$; the rate of change of the specific power of dissipation is $Q_0 \ddot{q}_0$. Hence it is interesting to investigate the dynamics of q_0, $\dot{q}_0$ and $\ddot{q}_0$.

From eqns (15), (22) and (60) and also the argument of never switching off in Theorem 1, we find the remarkable fact

$$\dot{q}_0 = \|\mathbf{c}\| x H(x - x_{\text{on}}). \tag{63}$$

That is, the coordinate x measures the dissipation power per unit generalized strain rate when $x \geqslant x_{\text{on}}$. Recall that x_{on} is the x-coordinate of the switch-on point. This formula renders us a vivid, global picture about the amount of the dissipation power at any point in the response subspace, as shown in Fig. 8(a). It can even be generalized to a more general path if x and $\dot{\mathbf{q}} = \mathbf{c}$ are interpreted appropriately.

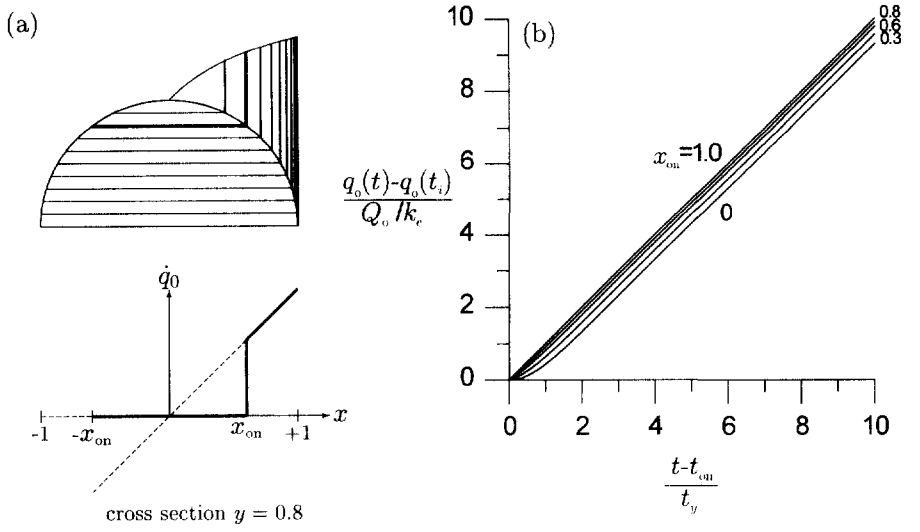

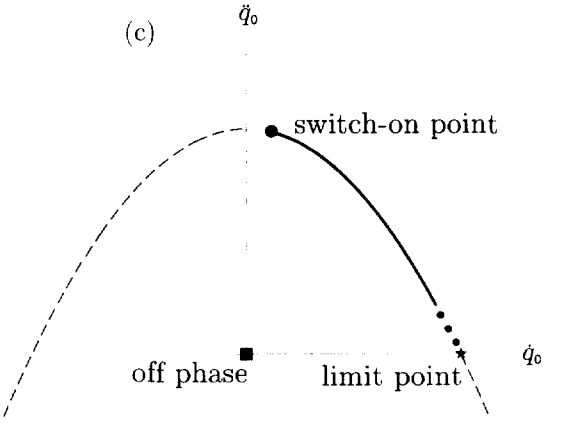

Fig. 8. Dissipation. (a) Dissipation power over the response subspace; (b) temporal growth of the work dissipated $Q_0 q_0$; (c) parabolic phase portrait of the dissipation 2-vector $(Q_0\dot{q}_0, Q_0\ddot{q}_0)$.

From eqns (33) and (9),

$$q_0(t) = q_0(t_i) + \frac{Q_0}{k_e} \ln [1 - H_1(t) + H_c(t) + x_{on} H_s(t)]. \tag{64}$$

The temporal growth of the specific work dissipated, $Q_0 q_0(t)$, for the perfect model subjected to the rectilinear path can be visualized by plotting $[q_0(t) - q_0(t_i)]/(Q_0/k_e)$ vs $(t - t_{on})/t_y$ for various values of x_{on}, $0 \leqslant x_{on} \leqslant 1$, as shown in Fig. 8(b). They are the curves for the logarithm of a $(\cosh + x_{on} \sinh)$ function. This figure depicts the dissipated work over the input subspace. Next, observe that eqn (45) indeed defines a parabola

$$\frac{k_e}{Q_0} [(\dot{q}_0)^2 - \|\mathbf{c}\|^2 H_1(t)] + \ddot{q}_0 = 0 \tag{65}$$

in the space $(\dot{q}_0, \ddot{q}_0)$ as shown in Fig. 8(c). However, only the first quadrant of the space is allowed due to the inequalities (47) and (49). The switch-on point $(\dot{q}_0(t_{on}), \ddot{q}_0(t_{on}))$ (or the initial point $(\dot{q}_0(t_i), \ddot{q}_0(t_i))$ if $t_{on} = t_i$) and the terminal point $(\dot{q}_0(t_f), \ddot{q}_0(t_f))$ (or the limit point

$(\bar{q}_0, 0)$ if $t_f = \infty$) are all located on the parabola of eqn (45) in the first quadrant, so that only the portion between the two points in the first quadrant may be present. Therefore, the dynamics of dissipation for the model and the path under consideration can be visualized in the first quadrant of the coordinate plane $(\dot{q}_0, \ddot{q}_0)$ as a path along the parabola starting at the switch-on point or at the initial point and leading to the limit point, which is located at the intersection point of the parabola and the $\dot{q}_0$-axis. In the off phase, the locus remains at the origin until the plasticity mechanism is switched on, whence it leaps to the parabola.

Now we return back to the three examples studied in Section 4, which have the same parabola and fixed point, since their $\|\mathbf{c}\|$'s are identical and their Q_0/k_e's are the same, too. In Fig. 4(f) we observe that the path of example 1 degenerates into one point, the fixed point $(\bar{q}_0, 0)$, since the switch-on point is just the fixed point for this example, while the paths of examples 2 and 3 coincide and look like a straight line because only small portions of the parabolas show them up.[16] Figure 4(d) and (e) shows that the curves of $\dot{q}_0$ and $\ddot{q}_0$ vs t, q_1, q_2 tend to the limit values $\bar{q}_0$ and 0, respectively, very soon for all generalized stress paths.

6.3. *Effect of generalized strain rates*

In order to study the effect of the constant generalized strain rate vectors $\mathbf{c}$ on the responses, we locate and fix the initial generalized stress point $\mathbf{Q}(t_i)$ on the yield hypersphere, i.e., $\mathbf{Q}(t_i)\cdot\mathbf{Q}(t_i) = Q_0^2$, and put the constant generalized strain rate vectors in all possible directions in the n-dimensional generalized stress space such that the initial direction cosine $\mathbf{Q}(t_i)\cdot\mathbf{c}/(\|\mathbf{Q}(t_i)\|\,\|\mathbf{c}\|)$, which equals x_i under the condition $|x_i| = x_{\text{on}}$ as is the present case, ranges from -1 to $+1$. For example, shown schematically in the inset of Fig. 9 are five examples which have identical initial points $\mathbf{Q}(t_i)$ marked by black solid circles in the figures but have five different orientations of $\mathbf{c}$, which generate limit strength points (or north poles) marked by stars. For a $\mathbf{c}$ oriented such that $-1 \leqslant x_i < 0$ it must belong to the case of first-off–then-on, and switch-on time is calculated via eqn (27). Therefore, we can evaluate the following:

$$\mathbf{Q}(t_{\text{on}}) = \mathbf{Q}(t_i) - 2x_i\bar{\mathbf{Q}},$$

$$\text{path arc-length up to } \mathbf{Q}(t_{\text{on}}) = \int_{t_i}^{t_{\text{on}}} \|\dot{\mathbf{Q}}(\xi)\|\,\mathrm{d}\xi = -2x_iQ_0,$$

$$\dot{q}_0(t_{\text{on}}) = \frac{\mathbf{Q}(t_{\text{on}})\cdot\mathbf{c}}{Q_0} \in [0, -x_i\|\mathbf{c}\|].$$

According to these formulae the switch-on curves, namely the curves of the switch-on point $\mathbf{Q}(t_{\text{on}})$ vs the direction cosine x_i, were plotted in Fig. 9(a)–(d) by dashed heavy lines. In addition, corresponding to every input of $\mathbf{c}$ the limiting state can be evaluated as follows:

$$\bar{\mathbf{Q}} = \frac{Q_0\mathbf{c}}{\|\mathbf{c}\|},$$

$$\text{path arc-length up to } \bar{\mathbf{Q}} = \begin{cases} -2x_iQ_0 + Q_0\arccos(-x_i) & \text{if } x_i < 0, \\ Q_0\arccos x_i & \text{if } x_i \geqslant 0, \end{cases}$$

$$\bar{q}_0 = \|\mathbf{c}\|.$$

According to these formulae the limit strength curves, namely the curves of the limit strength vector $\bar{\mathbf{Q}}$ vs the direction cosine x_i, are displayed in Fig. 9 by heavy solid lines. A solid light line marked with a particular symbol represents an isochronal response at a particular time instant identified by the symbol. In Fig. 9(a) and (b) the regions between the curves of $t = t_i + 2t_y$ and the north-pole curves are shaded to emphasize there are an infinite number of isochronal curves because the travel time needed to approach the limit

[16] Clearer images of the parabolic loci of this sort can be found in Fig. 10(h) and 11(c).

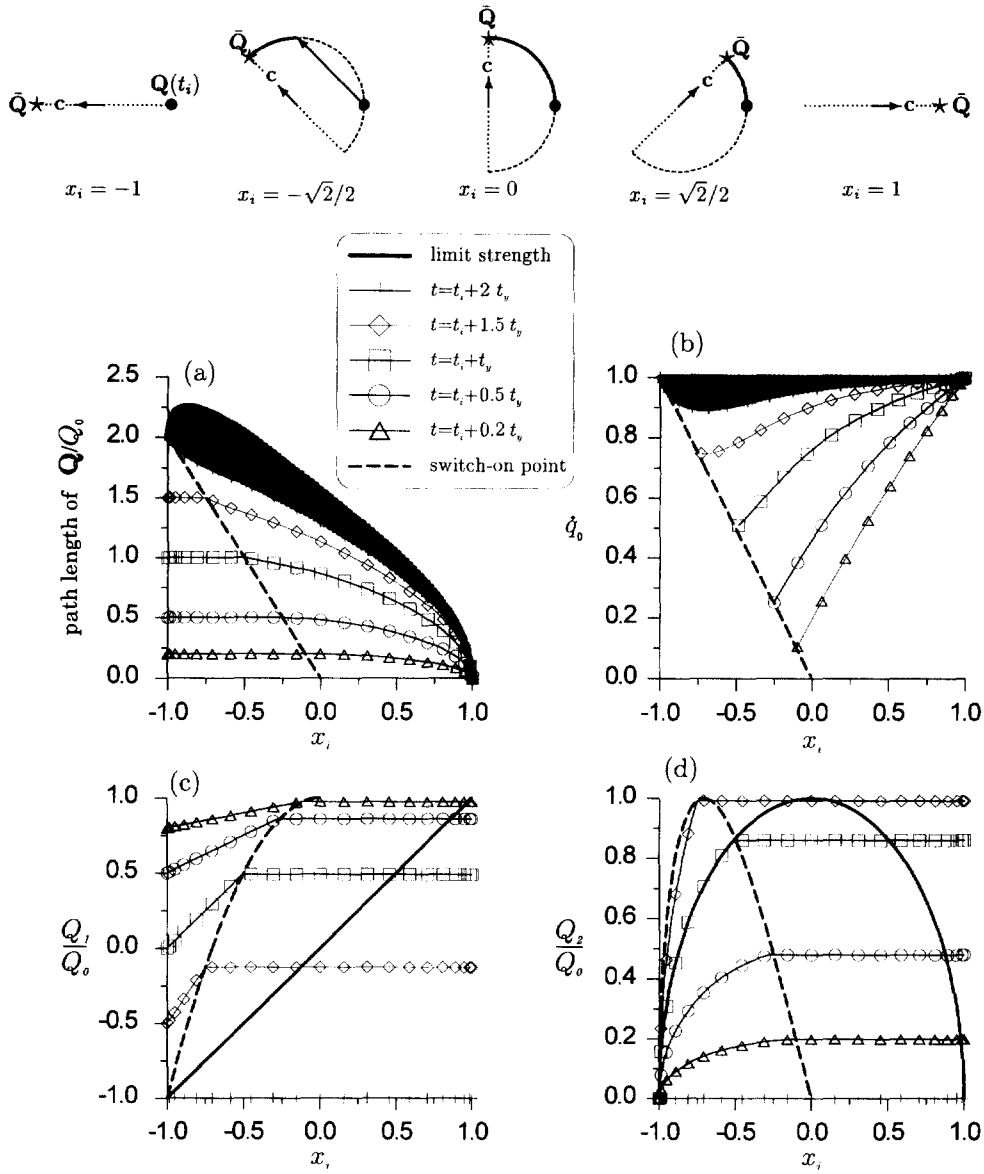

Fig. 9. Effect of orientations of generalized strain rates on: (a) path length of $\mathbf{Q}$; (b) $\dot{q}_0$; (c) Q_1; (d) Q_2.

strength is infinite. However, it is observed that after $2t_y$ the limit strength is not far away in general.

6.4. *Visualization for a more general input*

To offer insight through pictures and diagrams that can be drawn, we first approximate a continuous generalized strain path by a piecewise rectilinear path, yielding a sequence of $(\mathbf{c}^{(k)}, t_i^{(k)})$'s, of which piece k ($k = 1, 2, 3, \ldots$), runs with a constant rate $\mathbf{c}^{(k)}$ from time $t_i^{(k)}$ to time $t_i^{(k+1)}$. Then we move each $\mathbf{c}^{(k)}$ like a free vector to the origin of the generalized stress space, namely the center of the yield hypersphere, obtaining a limit strength vector $\bar{\mathbf{Q}}^{(k)}$ on the yield hypersphere, and also move to the initial point $\mathbf{Q}(t_i^{(k)})$, obtaining a switch-on point $\mathbf{Q}(t_{\text{on}}^{(k)})$ on the yield hypersphere if $t_i^{(k+1)} - t_i^{(k)}$ is long enough. Afterwards we draw a geodesic on the yield hypersphere $\mathbb{S}^{n-1}$ to connect the switch-on point $\mathbf{Q}(t_{\text{on}}^{(k)})$ to the limit strength point $\bar{\mathbf{Q}}^{(k)}$. The response path follows the geodesic to the limit strength point, close enough to it provided $t_i^{(k+1)} - t_i^{(k)}$ is long enough. In short, for each piece the response path is always "straight", following the shortest trail either in the generalized stress space $\mathbb{E}^n$ or

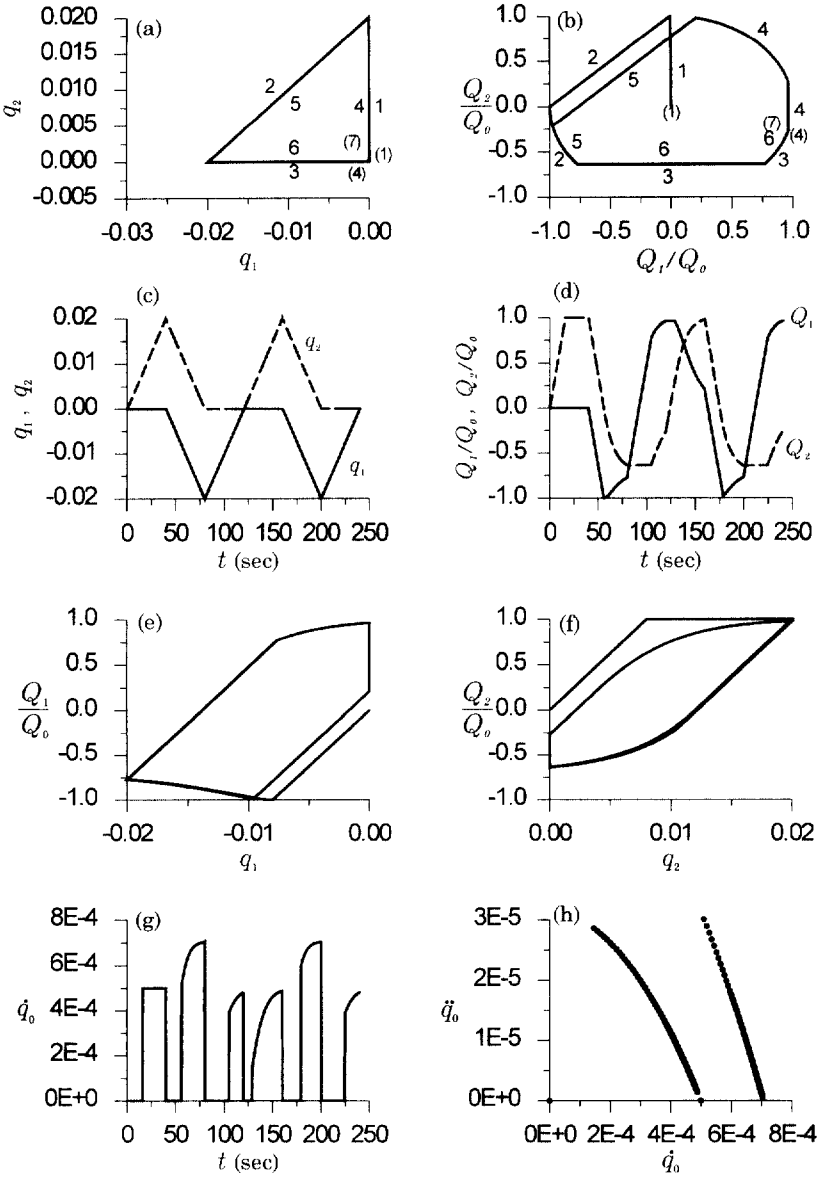

Fig. 10. Responses of the perfect elastoplastic model in two dimensions under a cyclic triangular generalized strain path. (a) Input of the generalized strain path; (b) output of the generalized stress path; time histories of (c) generalized strains and (d) generalized stress; hysteresis loops of (e) Q_1 vs q_1 and (f) Q_2 vs q_2; (g) time history of $\dot{q}_0$; and (h) phase portrait of dissipation.

on the yield hypersphere $\mathbb{S}^{n-1}$, and for each piece the speed of pace is constant in $\mathbb{E}^n$ but diminishes gradually on $\mathbb{S}^{n-1}$. In summary, according to the preceding study, for each piece there are three kinds of responses: (a) all-off: The piece k is all in the off (elastic) phase, the response path being straight as described by eqn (62) as $t_i^{(k)} < t_i^{(k+1)} \leqslant t_{\text{on}}^{(k)}$; (b) all-on: The piece k is all in the on (elastoplastic) phase, the response path being circular as described by eqn (62) as $t_{\text{on}}^{(k)} = t_i^{(k)} < t_i^{(k+1)}$; (c) first-off–then-on: The piece k is first in the off (elastic) phase and is then switched on at time $t_{\text{on}}^{(k)}$ predicted by eqn (27), the response path being first straight and then circular as described by eqn (62) as $t_i^{(k)} < t_{\text{on}}^{(k)} < t_i^{(k+1)}$. Be cautious that there is no case of first-on–then-off, as has been proved in Theorem 1.

In order to develop the geometrical visualization of the responses a two-dimensional example and a three-dimensional example are displayed in Figs 10 and 11, respectively. The inputs of the two cases are piecewise rectilinear generalized strain paths shown in Figs 10(a) and 11(a). The calculations were based on the formulae derived in Sections 3 and 4,

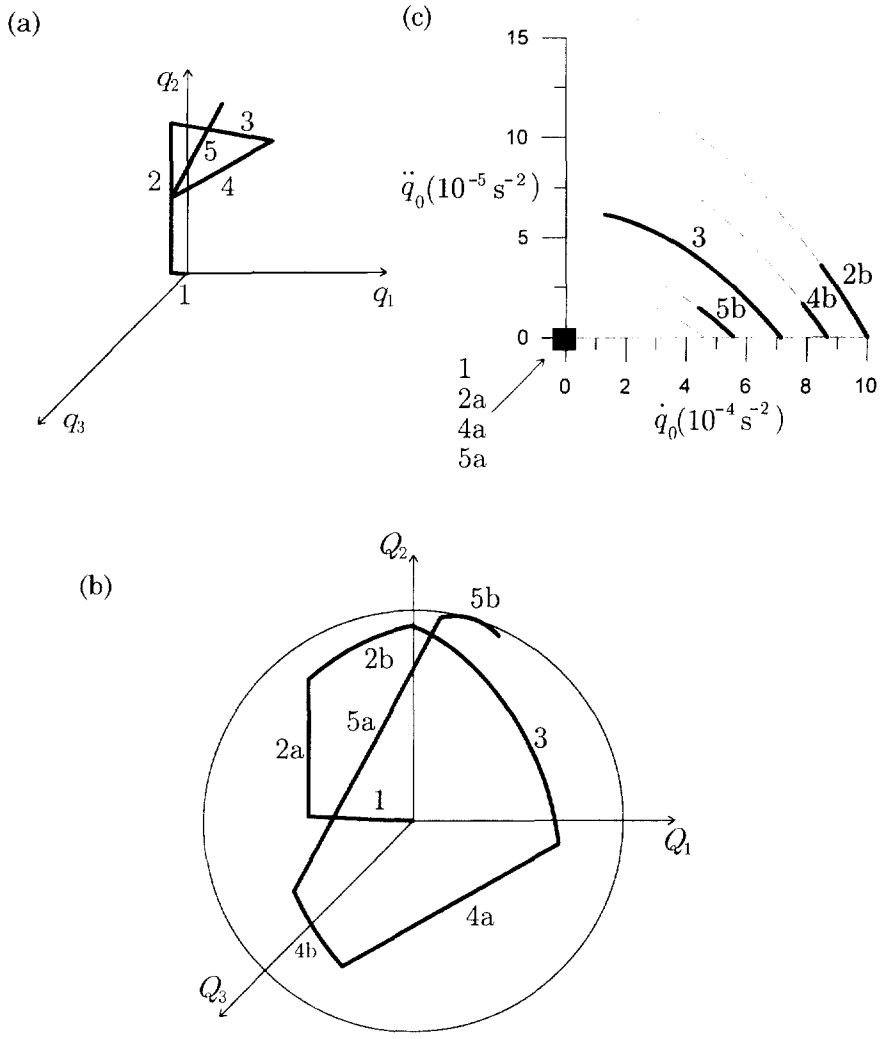

Fig. 11. Response of the perfect elastoplastic model in three dimensions. (a) Input of the generalized strain path; (b) output of the generalized stress path; (c) phase portrait of dissipation.

since the generalized strain paths are piecewise rectilinear, but the formulae are suitable for a single rectilinear generalized strain path with a specified initial generalized stress point so that in practical computation the global solution is obtained by piecing together the solutions of the consecutive pieces.

Figure 10 illustrates the response to an input of a cyclic triangular path in two dimensions, the first cycle of which consists of three pieces 1, 2 and 3. The second cycle consisting of pieces 4, 5 and 6 repeats in the generalized strain space the locus of the first cycle of pieces 1, 2 and 3, and so forth. Only the responses of the first two cycles are displayed because after those the responses were found to be almost repeated and stabilized. The results shown include the generalized stress path in Fig. 10(b), hysteresis loops in Fig. 10(e) and 10(f), time histories of generalized stresses in Fig. 10(c) and (specific) power of dissipation in Fig. 10(g), and phase portrait of $(\dot{q}_0, \ddot{q}_0)$ in Fig. 10(h). The response graph of the generalized stress path in Fig. 10(b) as can be seen is very different from the input graph of the generalized strain path in Fig. 10(a). One of two main features is that the generalized strain path is closed, but the corresponding generalized stress response has an open path. The points marked by (1), (4) and (7) in Fig. 10(a) are the same generalized strain points; however, the resulting generalized stress path 123456 as shown in Fig. 10(b) starts at, passes through and ends at three different generalized stress points marked by (1), (4) and (7), respectively. The other feature is that the generalized strain path is composed of straight

lines, but the corresponding generalized stress response has straight-line paths in the off phase but circular paths in the on phase.

Figure 11 illustrates the response to the input of a piecewise rectilinear path in three dimensions which consists of five pieces as shown in Fig. 11(a), marked consecutively by 1, 2, 3, 4 and 5. The resulting generalized stress path in three dimensions is shown in Fig. 11(b). The solid circle in Fig. 11(b) was the yield sphere $\mathbb{S}^2$. The piece marked by 1 was in the off phase; piece 2 was first-off–then-on, traversing a geodesic from the switch-on point to the corresponding limit strength point; piece 3 was totally in the on phase, tracing along another geodesic toward its own limit strength point; at the turning point of pieces 3 and 4 switching-off occurred upon initiating piece 4, and accordingly piece 4 was initially in the off phase and then in the on phase and marched along a geodesic toward its own limit strength point; similarly, at the end of piece 4 switching-off occurred upon initiating piece 5, which was also initially in the off phase and then in the on phase. Figure 11(c) displays the dissipation portrait as four heavy black squares (pieces 1, 2a, 4a and 5a) clustered at the origin and four heavy solid lines (pieces 2b, 3, 4b and 5b) in the first quadrant, where 2a represents the first part of piece 2 which is in the off phase and 2b represents the second part of piece 2 which is in the on phase, and so forth. As discussed in Subsection 6.2, the five pieces induce five parabolas, shown as dotted light lines in the figure. As time elapsed the dissipation portrait remained at the origin from time $t_i^{(1)}$ through $t_i^{(2)}$ to $t_{\text{on}}^{(2)}$, then suddenly at time $t_{\text{on}}^{(2)}$ leapt to the switch-on point of piece 2b following the second parabola defined by eqn (65) with $\mathbf{c}$ replaced by $\mathbf{c}^{(2)}$ in the direction indicated by the arrow, then at time $t_i^{(3)}$ jumped from the switch-off point of piece 2b to the switch-on point of piece 3, and so on. Note that the dissipation portrait did not visit the first parabola although it could be defined by eqn (65) with $\mathbf{c}$ replaced by $\mathbf{c}^{(1)}$.

Corresponding to the sequence of $(\mathbf{c}^{(k)}, t_i^{(k)})$, $k = 1, 2, 3, \ldots$, is a sequence of limit strength points $\bar{\mathbf{Q}}^{(k)}$, $k = 1, 2, 3, \ldots$, on the yield hypersphere. If we refine the approximation by decreasing all $(t_i^{(n+1)} - t_i^{(n)})$'s meanwhile increasing k and finally passing to the limit, the sequence of limit strength points becomes a north-pole curve $\bar{\mathbf{Q}} = \bar{\mathbf{Q}}(t)$, $t \geqslant t_i$ on the yield hypersphere, which is of class C^{s-1} if the generalized strain path $\mathbf{q} = \mathbf{q}(t)$, $t \geqslant t_i$ is of class C^s, $s = 1, 2, 3, \ldots$, but becomes disjointed at points where the path is continuous but not continuously differentiable. With these concepts we would be able to visualize the path of the response to a more general input.

7. ASYMPTOTIC BEHAVIOR

As the response to the input path with $\dot{\mathbf{q}} = \mathbf{c} \neq \mathbf{0}$, how soon will the generalized stress path reach the limit strength point $\bar{\mathbf{Q}} = Q_0 \mathbf{c}/\|\mathbf{c}\|$? It will take a finite time if the initial generalized stress point $\mathbf{Q}(t_i)$ satisfying

$$\mathbf{Q}(t_i) = x_i \bar{\mathbf{Q}}, \quad -1 \leqslant x_i \leqslant 1, \tag{66}$$

as was shown in example 1 of Fig. 4. For such a generalized stress path its switch-on point is just the limit strength point $\bar{\mathbf{Q}}$. Furthermore, by eqns (16), (22) and (37) we can evaluate $\dot{\mathbf{Q}} = k_e \mathbf{c} - (k_e/Q_0^2)(Q_0 \mathbf{c}/\|\mathbf{c}\|) \cdot \mathbf{c}(Q_0 \mathbf{c}/\|\mathbf{c}\|) = \mathbf{0}$ at this point. It means that, once switched on, the generalized stresses do not vary any more; even the journey along the rectilinear generalized strain path goes on without interruption. Thus with the particular initial generalized stress point specified by eqn (66), the switch-on point $\mathbf{Q}(t_{\text{on}})$ is just the fixed point $\bar{\mathbf{Q}}$ and it will take only a finite time $t_{\text{on}} - t_i$ to arrive at the fixed point $\bar{\mathbf{Q}} = \mathbf{Q}(t_{\text{on}})$. Otherwise, as was observed in examples 2 and 3 in Fig. 4, the generalized stress response would approach the limit strength points, but it would take infinite times to arrive at them, as to be analyzed in the following.

7.1. *Upper bound overall estimate*

It has been proved in Theorem 2 that for any specified rectilinear path (21) there exists a limit strength point $\bar{\mathbf{Q}}$ which is asymptotically stable. By using this fact we can prove:

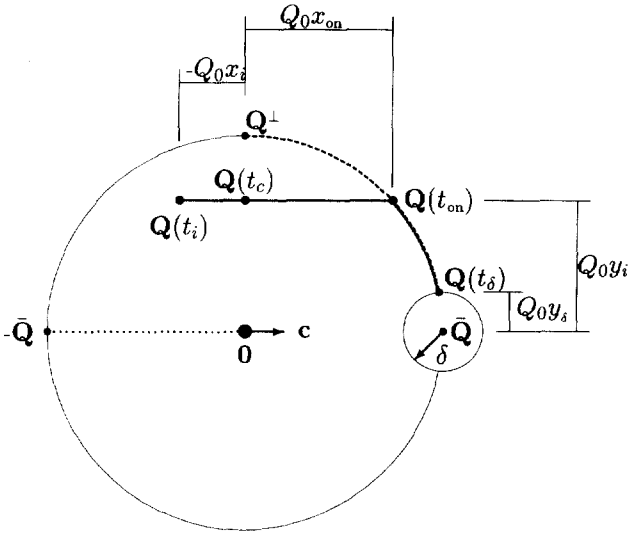

Fig. 12. The travel time along any geodesic path (solid line) is bounded by that of the dashed lines which amounts to the overall estimate.

Theorem 3. For any initial generalized stress point $\mathbf{Q}(t_i)$ confined by inequality (4), and any specified rectilinear generalized strain path (21) with $\dot{\mathbf{q}} = \mathbf{c} \neq \mathbf{0}$, there exists a time $t_\delta = t_\delta(\delta)$, $\delta > 0$, such that for all $t \geqslant t_\delta$ it must be $\|\mathbf{Q}(t) - \bar{\mathbf{Q}}\| \leqslant \delta$.

Proof: Given an admissible $\mathbf{Q}(t_i)$ and a nonzero $\mathbf{c}$, there are two possible cases: the two vectors are either linearly dependent or linearly independent. For the case $\mathbf{Q}(t_i)$ and $\mathbf{c}$ are linearly independent, we can find the four points: $\bar{\mathbf{Q}}$, $\mathbf{Q}^\perp$ and

$$\mathbf{Q}(t_c) = y_i \mathbf{Q}^\perp, \tag{67}$$

$$\mathbf{Q}(t_{on}) = x_{on}\bar{\mathbf{Q}} + y_i \mathbf{Q}^\perp, \tag{68}$$

where $\bar{\mathbf{Q}}$, $\mathbf{Q}^\perp$, y_i, x_{on} have been defined in eqns (37), (58), (25), and (26), respectively. For the case $\mathbf{Q}(t_i)$ and $\mathbf{c}$ are linearly dependent, as specified by eqn (66), we can pick an otherwise arbitrary vector $\mathbf{Q}^\perp$ such that $\|\mathbf{Q}^\perp\| = Q_0$ and $\mathbf{Q}^\perp \cdot \mathbf{c} = 0$, and set $y_i = 0$, so that the four points mentioned above can be found as well. Therefore, we need go no further into distinction between the two cases.

The travel time from $\mathbf{Q}(t_i)$ to $\mathbf{Q}(t_{on})$ is $t_{on} - t_i$, which is the sum of $t_{on} - t_c$ and $t_c - t_i$. Their upper bounds are estimated below: For any admissible initial point, $|t_c - t_i| \leqslant t_y$. Therefore, the upper bound of $t_c - t_i$ is t_y, which as defined in eqn (23) can be considered as the travel time from the south pole $-\bar{\mathbf{Q}}$ to the origin. To estimate the upper bound of $t_{on} - t_c$ compare the path of a straight line-segment (i.e., geodesic in $\mathbb{E}^n$) from $\mathbf{Q}(t_c)$ to $\mathbf{Q}(t_{on})$ with the path of a circular arc (i.e., geodesic in $\mathbb{S}^{n-1}$) from $\mathbf{Q}^\perp$ to the same point $\mathbf{Q}(t_{on})$ (cf Fig. 12). The travel time spent by the straight path from $\mathbf{Q}(t_c)$ to $\mathbf{Q}(t_{on})$ is

$$t_{on} - t_c = t_y x_{on}. \tag{69}$$

On the other hand, the circular arc path starting at $\mathbf{Q}^\perp$ at time say t_c is described by

$$\mathbf{Q}(t) = \tanh\frac{t - t_c}{t_y}\bar{\mathbf{Q}} + \operatorname{sech}\frac{t - t_c}{t_y}\mathbf{Q}^\perp \quad \forall\, t \geqslant t_c, \tag{70}$$

which is eqn (62) but with (x_i, y_i), t_i, x_{on} and t_{on} replaced by $(0, 1)$, t_c, 0 and t_c, respectively, since all in the on phase is the whole circular arc path which starts at time t_c at point $\mathbf{Q}^\perp$, which has the generalized coordinates $(0, 1)$. The arrival time, denoted by say t_m, at which

the circular arc path (70) arrives at $\mathbf{Q}(t_{on})$, is determined by equating the right-hand sides of eqns (68) and (70):

$$x_{on} = \tanh\frac{t_m - t_c}{t_y}, \quad y_i = \operatorname{sech}\frac{t_m - t_c}{t_y}.$$

The two equations generate the same solution

$$t_m = t_c + t_y \ln\sqrt{\frac{1+x_{on}}{1-x_{on}}} \tag{71}$$

upon noting eqns (26) and (27). It is easy to verify

$$x_{on} \leqslant \ln\sqrt{\frac{1+x_{on}}{1-x_{on}}},$$

so that from eqns (69) and (71) we have

$$t_{on} \leqslant t_m. \tag{72}$$

Substituting eqn (70) into the inequality $\|\mathbf{Q}(t) - \bar{\mathbf{Q}}\| \leqslant \delta$, we obtain

$$\left(\tanh\frac{t-t_c}{t_y} - 1\right)^2 + \left(\operatorname{sech}\frac{t-t_c}{t_y}\right)^2 \leqslant \left(\frac{\delta}{Q_0}\right)^2,$$

the real-valued solution of which is

$$t \geqslant t_c + t_y \ln\sqrt{\left(\frac{2Q_0}{\delta}\right)^2 - 1}. \tag{73}$$

This gives the arrival time after which the response path starting from point $\mathbf{Q}^{\perp}$ at time t_c will enter the δ-ball; it is the upper bound of the arrival time after which the response path starting at $\mathbf{Q}(t_c)$ will enter the δ-ball, according to the inequality (72). The upper bound for the whole path starting at $\mathbf{Q}(t_i)$ can now be obtained by adding t_y, the upper bound of $t_c - t_i$, as in the following:

$$t_\delta = t_i + t_y\left[1 + \ln\sqrt{\left(\frac{2Q_0}{\delta}\right)^2 - 1}\right]. \tag{74}$$

Therefore, it is concluded that for all admissible initial generalized stress vectors the generalized stress vectors at time $t \geqslant t_\delta$ must have already entered the δ-ball with center $\bar{\mathbf{Q}}$, i.e., $\|\mathbf{Q}(t) - \bar{\mathbf{Q}}\| \leqslant \delta$.

The above theorem asserts that within finite accuracy it takes a finite time for the response path to essentially reach the limit strength point $\bar{\mathbf{Q}}$. Equation (74) provides a formula for an upper bound estimate.

7.2. *Asymptoticity accounted for prestress*

The overall estimate given by eqn (74) is not dependent on the initial generalized stress vector $\mathbf{Q}(t_i)$. In this subsection we take prestress into account, deriving the exact formula for t_δ.

Given are a nonzero $\mathbf{c}$ and an otherwise arbitrary $\mathbf{Q}(t_i)$ which satisfies inequality (4). First, suppose $y_i \leqslant y_\delta$, where

$$y_\delta := \frac{\delta}{Q_0}\sqrt{1-\left(\frac{\delta}{2Q_0}\right)^2},$$

as shown in Fig. 12. Substituting eqns (37) and (62), where $t_i \leqslant t \leqslant t_{on}$, into the equality $\|\mathbf{Q}(t_\delta)-\bar{\mathbf{Q}}\| = \delta$, solving and considering inequality (4), we obtain

$$t_\delta = t_i + t_y\left[1-x_i-\sqrt{\left(\frac{\delta}{Q_0}\right)^2-y_i^2}\right]. \tag{75}$$

Next, consider $y_i > y_\delta$. Substituting eqns (37) and (62), where $t_i \leqslant t_{on} \leqslant t$, into the equality $\|\mathbf{Q}(t_\delta)-\bar{\mathbf{Q}}\| = \delta$, we obtain

$$\left[\frac{x_{on}\cosh\frac{t_\delta-t_{on}}{t_y}+\sinh\frac{t_\delta-t_{on}}{t_y}}{\cosh\frac{t_\delta-t_{on}}{t_y}+x_{on}\sinh\frac{t_\delta-t_{on}}{t_y}}\right]^2+y_i^2=\left(\frac{\delta}{Q_0}\right)^2.$$

The real-valued solution is found to be

$$t_\delta = t_{on}+t_y\ln\frac{y_i\sqrt{(2Q_0/\delta)^2-1}}{1+x_{on}}. \tag{76}$$

Then upon substituting eqns (27) and (26) for t_{on} and x_{on}, respectively, the formula becomes

$$t_\delta = t_i+t_y\left[\sqrt{1-y_i^2}-x_i+\ln\frac{y_i\sqrt{(2Q_0/\delta)^2-1}}{1+\sqrt{1-y_i^2}}\right], \tag{77}$$

which predicts the time at and after which the response path starting at point $\mathbf{Q}(t_i)$ at time t_i will reach and enter the δ-ball with center $\bar{\mathbf{Q}}$. Consequently, the following theorem can be delivered:

Theorem 4. For an initial generalized stress point $\mathbf{Q}(t_i)$ confined by inequality (4) and any specified rectilinear generalized strain path (21) with $\dot{\mathbf{q}} = \mathbf{c} \neq \mathbf{0}$, there exists a time $t_\delta = t_\delta(\delta, \mathbf{Q}(t_i))$ given by eqn (75) if $y_i \leqslant y_\delta$ and by eqn (77) if $y_i > y_\delta$ such that for all $t \geqslant t_\delta$ it must be $\|\mathbf{Q}(t)-\bar{\mathbf{Q}}\| \leqslant \delta$.

Define the dimensionless quantities

$$\hat{t}_\delta := \frac{t_\delta - t_i}{t_y}, \quad \hat{\delta} := \frac{\delta}{Q_0}. \tag{78}$$

The dimensionless travel time $\hat{t}_\delta$ refers to the travel time from the initial point to the δ-neighborhood of the limit point (i.e., somewhere close enough to the limit point within finite accuracy), but measured as a multiple of the yield time-scale. The normalized closeness number $\hat{\delta}$ indicates the closeness to the limit strength point as compared with the generalized yield stress; it is indeed the ratio of the radius of the δ-ball to that of the yield hypersphere. Equations (74), (75) and (77) can be nondimensionalized to

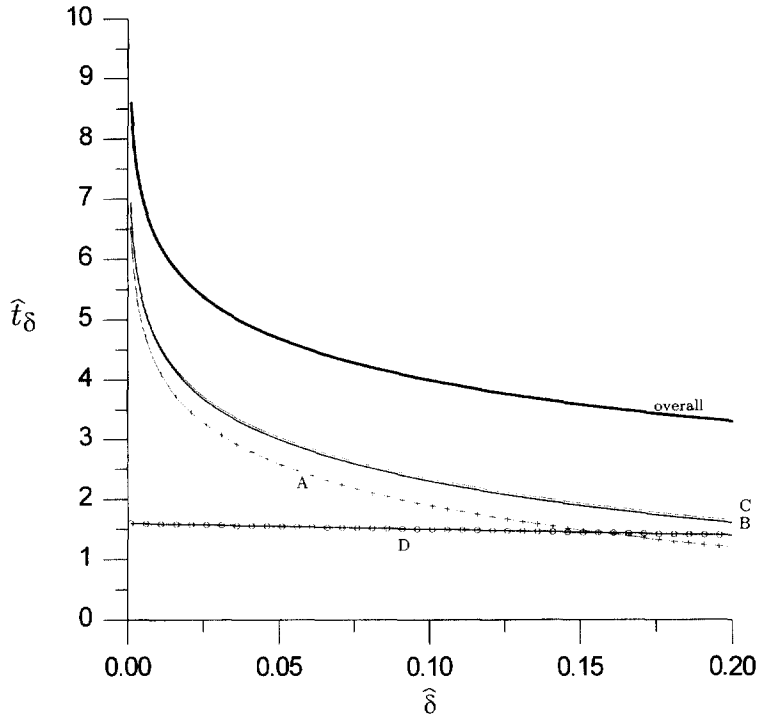

Fig. 13. Comparison of the travel times for different initial generalized stress points A, B, C and D, which are all bounded by the overall estimate.

$$\hat{t}_\delta = 1 + \ln \sqrt{(2/\hat{\delta})^2 - 1}, \tag{79}$$

$$\hat{t}_\delta = \begin{cases} 1 - x_i - \sqrt{\hat{\delta}^2 - y_i^2} & \text{if } y_i \leqslant y_\delta, \\ \sqrt{1 - y_i^2} - x_i + \ln \dfrac{y_i \sqrt{(2/\hat{\delta})^2 - 1}}{1 + \sqrt{1 - y_i^2}} & \text{if } y_i > y_\delta, \end{cases} \tag{80}$$

respectively. Figure 13 displays the variation of the travel time against the closeness to the limit strength point, comparing the upper bound overall estimate based on formula (79) with the exact values calculated from formula (80) for the four initial points with generalized coordinates (x_i, y_i): A (0.8, 0.6), B (0.6, 0.8), C (0, 0.4), and D (−0.6, 0). As expected, the upper bound overall estimate envelops the exact ones accounted for prestress. Figure 14 shows the effect of the initial generalized stresses by drawing isochronal lines. An isochronal line with a higher value demands a more travel time, namely a longer generalized strain path being needed to push the generalized stress path to approach its limit point. Four values of the normalized closeness $\hat{\delta} = 0.2, 0.1, 0.01$ and 0.001 are selected to demonstrate isochronal lines. In Fig. 14(a) the isochronal lines of the dimensionless travel times $\hat{t}_\delta = 2$, 1.5, 1.0, 0.5, 0.2 and 0 corresponding to $\hat{\delta} = 0.2$ are plotted, noticing that the line of $\hat{t}_\delta = 2$ is disconnected inside the admissible hypersphere whereas all the others are connected. For $\hat{t}_\delta = 0$ the curve is just the normalized δ-ball of the limit point. In Fig. 14(b) the isochronal lines of $\hat{t}_\delta = 3$, 2, 1, 0.5, 0.2 and 0 corresponding to $\hat{\delta} = 0.1$ are plotted, with the line of $\hat{t}_\delta = 3$ and 2 being disconnected within the admissible ball but the others being connected. In Fig. 14(c) the isochronal lines of $\hat{t}_\delta = 5$, 4.5, 4, 3.5, 3 and 0 corresponding to $\hat{\delta} = 0.01$ are plotted, all drawn lines disconnected within the admissible ball. In Fig. 14(d) the isochronal lines of $\hat{t}_\delta = 8$, 7.5, 7, 6.5 and 5 corresponding to $\hat{\delta} = 0.001$ are plotted, the five lines chosen being all disconnected inside the yield locus. It is observed that the smaller $\hat{\delta}$ is the larger $\hat{t}_\delta$ is required.

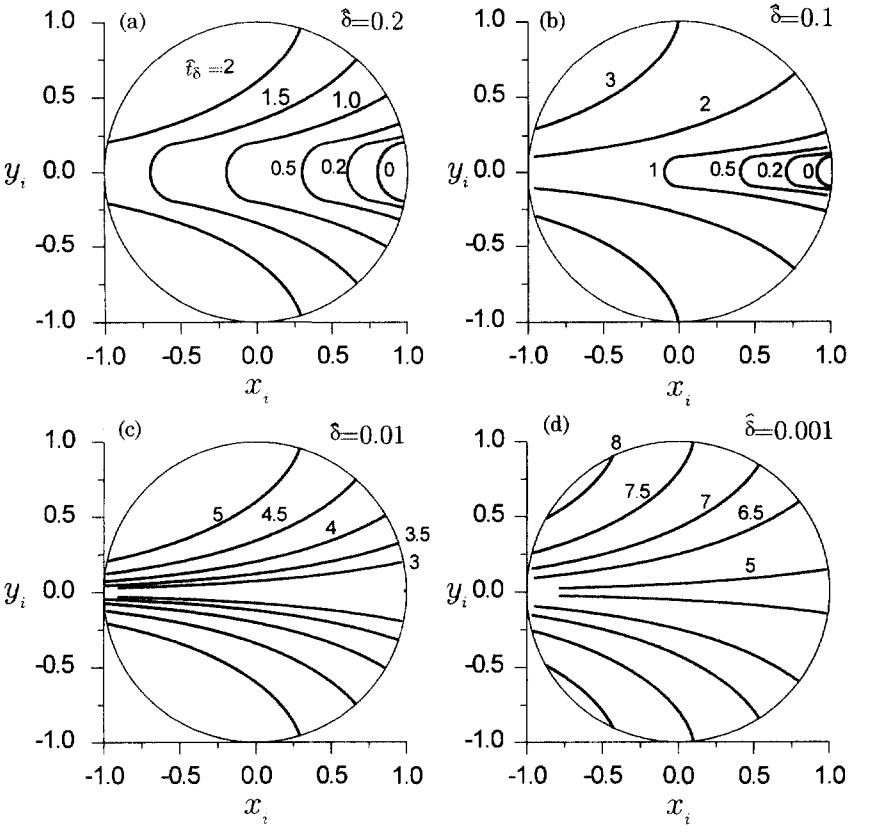

Fig. 14. Isochronal lines with various values of the dimensionless travel time $\hat{t}_\delta$ for different normalized closeness numbers: (a) $\hat{\delta} = 0.2$; (b)$\hat{\delta} = 0.1$; (c) $\hat{\delta} = 0.01$; (d) $\hat{\delta} = 0.001$.

8. CONCLUDING REMARKS

In this paper an effort to seriously use and rigorously analyze a system of axioms for plasticity has been made. The integrated utilization of the complementary trios and differential equations and the faithful treatment of initial conditions both deserve special attention. The complete solutions of the perfect elastoplastic model under rectilinear generalized strain paths include not only the on (elastoplastic) and off (elastic) solutions but also the formula for predicting the switch-on time and the assertion of never switching off. Geometrically speaking, the response path is a geodesic in the n-dimensional closed ball of generalized stresses, namely a straight line-segment in $\mathbb{E}^n$ and a great circular arc on $\mathbb{S}^{n-1}$. Based on them, we have established a geometrical approach, which appeals to intuitive thinking and can facilitate the construction of the path of response even to a sophisticated input. As observed, the perfect elastoplastic model goes by contraries, more than often exhibiting smooth generalized stress–strain curves as long as the generalized stress path extending on the yield hypersphere is still far away from the current limit strength point and keeps going to it.

It was found that the initial generalized stresses occupy a crucial position at the center of the stage in shaping the responses. The response behavior exhibited is far more diversified and plural than what was perceived before. The geometrical shapes of the generalized stress–strain curves were classified to be of totally ten types. The response generalized stress path and the response history of dissipated energy are of class C^0 and not C^1. It is a remarkable fact that in the response subspace the coordinate x measures the dissipation power per unit generalized strain rate when $x \geqslant x_{\text{on}}$, x_{on} being the x-coordinate of the switch-on point [see eqn (63) and Fig. 8(a)].

We have examined the long-term and asymptotic behavior. The existence of a limit and fixed point of a rectilinear generalized strain path was proved by the use of Lyapunov's

Table 1. Control parameters

Space		Parameters
Initial values	$\mathbf{Q}(t_i)$	x_i, y_i
Input paths	Direction $\mathbf{c}/\|\mathbf{c}\|$	x_t
	size $\|\mathbf{c}\|$	t_s
Property constants	k_e, Q_0	
Asymptotic behavior	δ	$\hat{\delta}$

direct method, which was also utilized to verify that the fixed point is asymptotically stable, so that the existence of a point attractor was thus confirmed. We have derived the formulae of closeness to the limit strength point and identified the factors of influence. The dependence of the responses on the product space mentioned in Section 1 has been thoroughly investigated with control parameters identified, which are summarized in Table 1.

Acknowledgment—The financial support provided by the National Science Council under Grant NSC 85-2211-E-002-001 is gratefully acknowledged.

REFERENCES

Das, A. (1993) *The Special Theory of Relativity: A Mathematical Exposition*. Springer-Verlag, New York.
Doughty, N. A. (1990) *Lagrangian Interaction: An Introduction to Relativistic Symmetry in Electrodynamics and Gravitation*. Addison-Wesley, Sydney.
Hirsch, M. W. and Smale, S. (1974) *Differential Equations, Dynamical Systems, and Linear Algebra*. Academic Press, New York.
Hong, H.-K. and Liou, J.-K. (1993) Integral-equation representations of flow elastoplasticity derived from rate-equation models. *Acta Mechanica* **96,** 181–202.
Hong, H.-K. and Liu, C.-S. (1993) Reconstructing J_2 flow model for elastoplastic materials. *Bulletin of the College of Engineering, National Taiwan University* **57,** 95–114.
Hong, H.-K. and Liu, C.-S. (1997a) Prandtl-Reuss elastoplasticity: on-off switch and superposition formulae. *International Journal of Solids and Structures* **34,** 4281–4304.
Hong, H.-K. and Liu, C.-S. (1997b) Minkowski spacetime and Lorentz group of perfect elastoplasticity, submitted.
Krieg, R. D. and Krieg, D. B. (1977) Accuracies of numerical solution methods for the elastic-perfectly plastic model. *Journal of Pressure Vessel Technology ASME* **99,** 510–515.
Kuksin, S. B. (1996) On classical solutions of the Prandtl-Reuss equations of perfect elastoplasticity. *Proceedings of the Royal Society of Edinburgh* **126A,** 1297–1308.
Lubliner, J. (1990). *Plasticity Theory*. Macmillan, New York.
Lyapunov, A. M. (1992) General problem of stability of motion, translated by A. T. Fuller. *International Journal of Control* **55,** 531–773.
Martin, J. B. (1975) *Plasticity: Fundamentals and General Results*. MIT Press, Cambridge, Mass.
Prager, W. (1956) General theory of limit design. *Proceedings of the 8th International Congress of Applied Mechanics* (Istanbul, 1952), Istanbul, **2,** 65–72.
Prager, W. (1959) *An Introduction to Plasticity*. Addison-Wesley, Reading, Mass.
Smale, S. (1967) Differential dynamical systems. *Bulletin of the American Mathematical Society* **73,** 747–817.
Thompson, J. M. T. and Stewart, H. B. (1993) A tutorial glossary of geometrical dynamics. *International Journal of Bifurcation and Chaos* **3,** 223–239.

APPENDIX

In this Appendix we give a detailed analysis and make a further classification of case (III) of the generalized stress–strain curves discussed in Section 5. First, we study the slopes of the curves. From eqns (8), (22) and (54) we have

$$\dot{Q}_k(t) = k_e c_k - \frac{\dot{Y}(t)}{Y(t)} \frac{Q_k(t_i) + k_e c_k \left\{ \dfrac{q_l - q_l(t_i)}{c_l} [1 - H_1(t)] + t_y [-x_t H_1(t) + x_{on} H_c(t) + H_s(t)] \right\}}{1 - H_1(t) + H_c(t) + x_{on} H_s(t)}, \tag{A1}$$

where $\dot{Y}/Y$ can be calculated through eqns (33) and (34) by

$$\frac{\dot{Y}(t)}{Y(t)} = \frac{x_{on} H_c(t) + H_s(t)}{t_s [1 - H_1(t) + H_c(t) + x_{on} H_s(t)]}. \tag{A2}$$

Hence

$$\dot{Q}_k(t) = k_e c_k - \frac{x_{on}H_c(t) + H_s(t)}{t_y[1 - H_1(t) + H_c(t) + x_{on}H_s(t)]}$$
$$\frac{Q_k(t_i) + k_e c_k \left\{\dfrac{q_l - q_l(t_i)}{c_l}[1 - H_1(t)] + t_y[-x_i H_1(t) + x_{on}H_c(t) + H_s(t)]\right\}}{1 - H_1(t) + H_c(t) + x_{on}H_s(t)}. \tag{A3}$$

In the off phase the slope is constant; however, in the on phase it was known in Section 4 that the slope is varying and tends to zero as t approaches infinity. Therefore, we want to know whether there exist other zeros of the slope or not. For this purpose we study eqn (A3) in the on phase, for which the finding of zeros is equivalent to solving the following equation:

$$k_e c_k - \frac{x_{on}H_c(t) + H_s(t)}{t_y[1 - H_1(t) + H_c(t) + x_{on}H_s(t)]}$$
$$\frac{Q_k(t_i) + k_e c_k \left\{\dfrac{q_l - q_l(t_i)}{c_l}[1 - H_1(t)] + t_y[-x_i H_1(t) + x_{on}H_c(t) + H_s(t)]\right\}}{1 - H_1(t) + H_c(t) + x_{on}H_s(t)} = 0. \tag{A4}$$

Taking $t > t_{on}$ and using eqn (34) we obtain

$$k_e c_k - \frac{x_{on}\cosh\dfrac{t - t_{on}}{t_y} + \sinh\dfrac{t - t_{on}}{t_y}}{t_y\left[\cosh\dfrac{t - t_{on}}{t_y} + x_{on}\sinh\dfrac{t - t_{on}}{t_y}\right]}$$
$$\frac{Q_k(t_i) + k_e c_k t_y\left[-x_i + x_{on}\cosh\dfrac{t - t_{on}}{t_y} + \sinh\dfrac{t - t_{on}}{t_y}\right]}{\cosh\dfrac{t - t_{on}}{t_y} + x_{on}\sinh\dfrac{t - t_{on}}{t_y}} = 0. \tag{A5}$$

Expanding the above equation and dividing by $k_e c_k t_y$, we obtain

$$\left[\cosh\frac{t - t_{on}}{t_y} + x_{on}\sinh\frac{t - t_{on}}{t_y}\right]^2 - \left[x_{on}\cosh\frac{t - t_{on}}{t_y} + \sinh\frac{t - t_{on}}{t_y}\right]$$
$$\left[\frac{Q_k(t_i)}{k_e c_k t_y} - x_i + x_{on}\cosh\frac{t - t_{on}}{t_y} + \sinh\frac{t - t_{on}}{t_y}\right] = 0. \tag{A6}$$

After some manipulations we have

$$1 - x_{on}^2 - \left[\frac{Q_k(t_i)}{k_e c_k t_y} - x_i\right]\left[x_{on}\cosh\frac{t - t_{on}}{t_y} + \sinh\frac{t - t_{on}}{t_y}\right] = 0. \tag{A7}$$

It is a quadratic algebraic equation for $\exp[(t - t_{on})/t_y]$ as follows:

$$\left(\frac{Q_k(t_i)}{k_e c_k t_y} - x_i\right)(1 + x_{on})(\exp[(t - t_{on})/t_y])^2 - 2[1 - x_{on}^2]\exp[(t - t_{on})/t_y] - \left(\frac{Q_k(t_i)}{k_e c_k t_y} - x_i\right)(1 - x_{on}) = 0. \tag{A8}$$

Because $0 \leqslant x_{on} < 1$ the first and last coefficients possess different signs, so if the solution exists take only the positive one. The following condition:

$$1 - x_{on}^2 + \left(\frac{Q_k(t_i)}{k_e c_k t_y} - x_i\right)^2 > 0$$

is always true under the given condition, so that the solution of eqn (A8) is found to be

$$\exp[(t - t_{on})/t_y] = \frac{1 - x_{on}^2 \pm \sqrt{[1 - x_{on}^2]^2 + \left(\dfrac{Q_k(t_i)}{k_e c_k t_y} - x_i\right)^2(1 - x_{on}^2)}}{\left(\dfrac{Q_k(t_i)}{k_e c_k t_y} - x_i\right)(1 + x_{on})} \quad \text{if} \quad \frac{Q_k(t_i)}{k_e c_k t_y} - x_i \gtrless 0. \tag{A9}$$

The following conditions:

$$\text{if} \quad \frac{Q_k(t_i)}{k_e c_k t_y} - x_i > 0, \quad x_{on}^2 + \left(\frac{Q_k(t_i)}{k_e c_k t_y} - x_i\right) x_{on} - 1 < 0; \tag{A10}$$

$$\text{if} \quad \frac{Q_k(t_i)}{k_e c_k t_y} - x_i < 0, \quad x_{on}^2 + \left(\frac{Q_k(t_i)}{k_e c_k t_y} - x_i\right) x_{on} - 1 > 0 \tag{A11}$$

are required for the solution of t to satisfy $t > t_{on}$. But the two inequalities in eqn (A11) contradict each other due to $0 \leqslant x_{on} < 1$; hence only the statement in eqn (A10) is valid. Consequently, under the following conditions the curve possesses a peak or a trough:

$$\frac{Q_k(t_i)}{k_e c_k t_y} - x_i > 0, \quad x_{on}^2 - \left(x_i - \frac{Q_k(t_i)}{k_e c_k t_y}\right) x_{on} - 1 < 0, \tag{A12}$$

for which the peak or trough occurs at the time instant

$$t_s = t_{on} + t_y \ln \frac{1 - x_{on}^2 + \sqrt{[1 - x_{on}^2]^2 + \left(\frac{Q_k(t_i)}{k_e c_k t_y} - x_i\right)^2 (1 - x_{on}^2)}}{\left(\frac{Q_k(t_i)}{k_e c_k t_y} - x_i\right)(1 + x_{on})}. \tag{A13}$$

It can be seen from the above analyses that the three parameters $Q_k(t_i)/(k_e c_k t_y)$, x_i and x_{on} play the key role in shaping the geometrical forms of generalized stress–strain curves. The inequalities in eqn (A12) together with $0 \leqslant x_{on} < 1$ and $-x_{on} \leqslant x_i \leqslant x_{on}$ constitute the necessary and sufficient conditions for a response curve of generalized stress versus generalized strain to possess a peak or a trough. We set $t = t_{on}$ in eqn (A3) to obtain

$$\dot{Q}_k(t_{on}) = k_e c_k - \frac{x_{on} Q_k(t_i) + k_e c_k t_y (x_{on} - x_i) x_{on}}{t_y}. \tag{A14}$$

The derivative in the above must be understood as the right derivative at $t = t_{on}$. Now consider the two cases $c_k > 0$ and $c_k < 0$ to delimit the regions of $\dot{Q}_k(t_{on}) > 0$ and $\dot{Q}_k(t_{on}) < 0$. For the case $c_k > 0$ the region of $\dot{Q}_k(t_{on}) > 0$ is enclosed by the following inequalities:

$$x_{on}^2 - \left(x_i - \frac{Q_k(t_i)}{k_e c_k t_y}\right) x_{on} - 1 < 0, \quad \frac{Q_k(t_i)}{k_e c_k t_y} - x_i < 0, \quad 0 \leqslant x_{on} < 1, \quad -x_{on} \leqslant x_i \leqslant x_{on}. \tag{A15}$$

And the region of $\dot{Q}_k(t_{on}) < 0$ is enclosed by the following inequalities:

$$x_{on}^2 - \left(x_i - \frac{Q_k(t_i)}{k_e c_k t_y}\right) x_{on} - 1 > 0, \quad \frac{Q_k(t_i)}{k_e c_k t_y} - x_i > 0, \quad 0 \leqslant x_{on} < 1, \quad -x_{on} \leqslant x_i \leqslant x_{on}. \tag{A16}$$

For the case $c_k < 0$ the region of $\dot{Q}_k(t_{on}) > 0$ is enclosed by the following inequalities:

$$x_{on}^2 - \left(x_i - \frac{Q_k(t_i)}{k_e c_k t_y}\right) x_{on} - 1 > 0, \quad \frac{Q_k(t_i)}{k_e c_k t_y} - x_i > 0, \quad 0 \leqslant x_{on} < 1, \quad -x_{on} \leqslant x_i \leqslant x_{on}. \tag{A17}$$

And the region of $\dot{Q}_k(t_{on}) < 0$ is enclosed by the following inequalities:

$$x_{on}^2 - \left(x_i - \frac{Q_k(t_i)}{k_e c_k t_y}\right) x_{on} - 1 < 0, \quad \frac{Q_k(t_i)}{k_e c_k t_y} - x_i < 0, \quad 0 \leqslant x_{on} < 1, \quad -x_{on} \leqslant x_i \leqslant x_{on}. \tag{A18}$$